Understanding Individual Motion Sickness Susceptibility

The Roles of Rotational Motion Perception and Postural Stability

Thesis

T.M.K. Coutuer

Delft University of Technology

Understanding Individual Motion Sickness Susceptibility

The Roles of Rotational Motion Perception and Postural Stability

by

T.M.K. Coutuer

To obtain the degree of Master of Science
at the Delft University of Technology,
to be defended publicly on 26 June 2026.

Student number:	5001196
Supervisors:	Dr.ir. R. Happee, Dr.ir. V. Kotian
Faculty:	CoR, Mechanical Engineering, Delft
Thesis committee:	Dr.ir. R. Happee, Dr.ir. V. Kotian & Dr.ir. D.M. Pool

Cover:	Rotational seat at the faculty of Mechanical Engineering at TU Delft
Style:	TU Delft Report Style, with modifications by Tine Coutuer

Abstract

The development of automated vehicles is progressing rapidly. This comes with numerous benefits, including increased safety, accessibility, and productivity, as well as reduced emissions and traffic. However, many challenges remain. One of the drawbacks is increased susceptibility to motion sickness due to the lack of control and the inability to anticipate motion as a passenger.

Motion sickness is a complex phenomenon generally believed to be influenced by sensory conflict; however, it is increasingly recognized as involving postural stability and head-neck stabilization. Despite extensive research on motion sickness, many studies examine motion perception and postural stability in isolation, without considering their interaction. Furthermore, while it is known that sensory reliance and motor strategies are individually dependent, this is rarely incorporated in existing models.

In this thesis, these gaps will be addressed by employing an experimental approach to investigate the relationships among individual differences in rotational motion perception, postural stability, and sensitivity to motion sickness. This is achieved by performing a structured experiment in which participants are exposed to dynamic motion while their postural sway, motion perception, dynamic head stabilization, and susceptibility to motion sickness are examined.

A significant positive correlation was found between the velocity storage time constant and motion sickness severity (ρ = 0.528, p = 0.012), suggesting that the EVAR paradigm may serve as a prescreening method for motion sickness susceptibility. No significant correlation was found between motion sickness severity and postural sway or dynamic stabilization, suggesting that these measures may not be appropriate to screen individuals for motion sickness susceptibility.

Preface

I chose this topic for my thesis as it sounded interesting and straightforward, and I thought it would be fun to conduct an experiment and possibly make people sick. However, the road towards the end of this thesis was not always as smooth as I had anticipated. There were chairs that didn't rotate the way I wanted, sensors that stopped sensing whenever, and data that caused late-night headaches. Still, these problems and frustrations taught me to be even more patient and flexible and to accept situations beyond my control.

During this process, I was greatly supported and would therefore like to thank my supervisor, Professor Riender Happee, for his encouragement and guidance, and for lifting my spirits when I felt lost. I would also like to thank Dr. Varun Kotian for guiding me throughout this process, sharing his knowledge on the topic, and allowing me to be part of his research.

I also want to thank my fellow master's students, who spent almost every day with me over the last two years. We have shared laughter, life questions, achievements, complaints, stress, and a lot of cheap coffee. Thank you, Frederick, Matthias, and Maxim, for helping me through the whole adventure. And of course, all the other *strijders*, who, every quarter, fought with us at the doors of the Library at 7.50 a.m. and made the study breaks even more enjoyable. Lastly, thank you to my girlzz at home for letting me be their favorite forever student.

I would also like to thank all my housemates over the last six years in Delft, both at the Bronx and Balpol, for giving me a safe and familiar place to return to at the end of the day. Thank you, Emiel, Frederic, Wout, Tim, Evert, Loes, Maxim, Rune, Bram, and Antra. A big shoutout as well to everyone in Moeder Delftsche for giving me an unforgettable six years in Delft. Lastly, I want to give an extra thanks to Emiel, who has been my mental support and private tutor since the day I arrived in Delft.

And of course, a very big thank you to my family. Thank you, Rosalie and Rob, who had to live in my shadow for their whole lives and handled it with admirable strength. Most importantly, a golden medal should be given to my parents for giving me every opportunity in life and for supporting me, both mentally and financially, through every decision I made. I would not have come this far without you.

With this thesis, I close a challenging, chaotic, but beautiful chapter of my life. It was not always easy, but it was definitely memorable and absolutely worth it. And, in the legendary words of Pitbull: "*Believe me, been there, done that, but every day above ground is a great day, remember that!*"

Thank you.

T.M.K Coutuer

Contents

List of Figures

Nomenclature

Abbreviation	Definition
AP	Anteroposterior
AVs	Automated Vehicles
DAVSi	Delft Advanced Vehicle Simulator
CCW	Counterclockwise
CCR	Cervicocollic Reflex
CV	Coefficient of Variation
CW	Clockwise
EC	Eyes Closed
EO	Eyes Open
EVAR	Earth Vertical Axis Rotation
fApEn	fuzzy approximate entropy
HREC	Human Research Ethics Committee
MCA	Motion Cueing Algorithm
MISC	Misery Scale
ML	Mediolateral
MPC	Model Predictive Control
MS	Motion Sickness
MSSQ	Motion Sickness Susceptibility Questionnaire
MSAQ	Motion Sickness Assessment Questionnaire
MV	Mean Velocity
PRV	Perceived Rotational Velocity
SD	Standard Deviation
SPV	Slow-Phase Eye Velocity
TPL	Total Path Length
VCR	Vestibulocollic Reflex

1

Introduction

The development of automated vehicles (AVs) is progressing rapidly and is expected to fundamentally transform road transportation. AVs promise numerous benefits, including increased safety, reduced congestion, improved accessibility, and more productive use of travel time. However, despite these advantages, automated vehicles also introduce new challenges. Besides legal, ethical, and privacy concerns, the transition from active driver to passive passenger affects how vehicle motion is perceived and anticipated [Martínez-Díaz and Soriguera, 2018].

One of the key motivations behind the development of automated vehicles is their potential to improve road safety. The World Health Organization estimated that worldwide, every year, 1.19 million people die as a result of road traffic crashes, and about 20 to 50 million more suffer from non-fatal injuries, often leading to a disability [WHO, 2023]. Furthermore, a study in the United States estimated that 94% of motor vehicle accidents are caused by driver error, ranging from decision and recognition errors to driving while intoxicated or drowsy, all of which severely affect drivers' reaction time and the overall safety of road users [LawInfo Staff, 2024]. By removing the driver from the loop in AVs, human error can be significantly reduced or even eliminated. However, while automation may improve safety, it also introduces new comfort and usability challenges, especially due to reduced control and an inability to anticipate motion.

Motion sickness (MS) is a phenomenon that occurs as a consequence of perceived self-motion and orientation cues. The brain continuously receives information from the vestibular and visual systems. When the brain receives mismatched information, a sensory conflict is created [Sherman, 2006]. It is found that symptoms most likely occur at frequencies around 0.16 Hz, and these may occur in both real vehicles and virtual environments, such as fixed-base or automobile simulations, as well as virtual-reality headsets. In virtual environments, this conflict arises because the visual system receives motion cues while the vestibular system detects little or no corresponding movement [Chang et al., 2020]. This kind of motion sickness can be referred to as virtual-induced motion sickness [Bos and Bles, 1998]. Although motion sickness does not usually cause permanent health issues, it may affect people's capacity to safely carry out physical or mental tasks, which can lead to dangerous situations [Stoffregen and Smart, 1998].

Other theories suggest that motion sickness is not only a sensory conflict phenomenon, but also a postural control problem. Riccio and Stoffregen (1991) defined postural stability as "the state in which uncontrolled movements of the perception and action systems are minimized". In this context, postural instability does not imply a total loss of movement control or balance, but rather a reduced ability to stabilize the body to perturbation [Riccio and Stoffregen, 1991].

In addition to the stability of the whole body, stabilizing the head and neck is crucial for maintaining gaze and orientation during motion. To achieve this, a combination of voluntary motor control, passive mechanical properties, and muscle control strategies is required. Failing to maintain head and neck stabilization can amplify sensory mismatch and aggravate motion sickness symptoms. The ability to stabilize the head and neck varies significantly with age, experience, and training. This is why a trained

athlete will show better postural stability control [Keshner, 2000]. Understanding the relationship between postural control, head-neck stabilization, and motion sickness can help identify individuals who are more vulnerable to it. This knowledge may help adapt AVs and virtual environments, accordingly, to limit the negative effects.

Despite a large amount of research already performed on the topic of motion sickness, many studies examine these factors in isolation, focusing exclusively on motion perception, postural stability, or dynamic head stabilization, without considering their interactions. Furthermore, while it is known that sensory reliance and motor strategies are individually dependent, this is rarely incorporated in existing models. Additionally, a tool is lacking to quickly assess a person's susceptibility to motion sickness based on indicators such as postural sway, motion perception, and stabilization effort. These are important, as understanding individual susceptibility will enable the development of adaptive systems and personalized mitigation strategies, increasing user acceptance of AVs and VR environments.

To address these research gaps, this thesis will investigate the relationship among individual differences in postural stability and rotational motion perception, and their correlation with sensitivity to motion sickness. By quantifying these relationships, the goal is to identify measurable predictors of individual motion sickness susceptibility. To reach this goal, a structured experiment is conducted where participants are subjected to controlled movement while being monitored.

This thesis is structured as follows. Chapter 2 reviews relevant literature on motion sickness, postural control, and motion perception. Chapter 3 presents the objectives and the hypotheses. Chapter 4 discusses the experimental outline, followed by the analysis and results in Chapter 5. Finally, the findings are discussed in Chapter 6, where limitations, implications, and the conclusion are included.

2

Related work

Susceptibility to motion sickness refers to the likelihood of a person experiencing symptoms of MS. It has been found that some people are more prone to motion sickness than others. This susceptibility depends on multiple distinct factors, including age, sex, genetics, vestibular sensitivity, and personal traits. For example, a higher susceptibility has been observed in women in general, and it begins in children around age 7, peaking around age 10. Older people seem to experience less sensitivity to motion sickness, or may avoid motion more often if they are aware of their sensitivity. Furthermore, people with a history of migraines or vestibular disorders tend to be more sensitive [Golding, 2006].

Previous research has shown that drivers experience significantly less motion sickness than passengers, both in simulation and in real-life scenarios. The difference in susceptibility is that passengers cannot control the movement itself. As drivers can actively anticipate and influence motion, this reduces sensory conflict and increases predictability [Olnick and Lubow, 1991].

Many studies have already been done on topics such as postural stability, motion perception and motion sickness. However, only a few studies measure these aspects in the same participants and evaluate their relation. Irmak et al. (2021) performed an experiment on the Earth Vertical Axis Rotation (EVAR) motion paradigm, in which a subject sitting upright is rotated around the Earth's vertical yaw axis [Irmak et al., 2021]. At the start of the rotation, the semicircular canals are stimulated, and they detect the angular acceleration. During constant rotation, the fluid in the canals catches up, and the perception of rotation gradually decreases. Once the rotation stops, the fluid moves in the opposite direction, and the subject perceives motion, even if the chair is stationary. In the current experiment, the *velocity storage time constant* is recorded as the time constant describing the decay of perceived rotation after the motion stops. A related experiment was conducted by Bertolini et al. (2011), who simultaneously measured slow-phase eye velocity (SPV) and perceived rotational velocity (PRV) after a sudden stop from yaw rotations at constant velocity. They fitted both responses with the two exponential functions with different time constants. They found that SPV and PRV share the same underlying velocity storage time constant. They state that the velocity storage time constants in healthy humans typically range from 10 to 30 seconds [Bertolini et al., 2011].

Some past literature claims that people with greater velocity storage time constants have higher motion sickness susceptibility, though the research has been inconsistent. Irmak et al. (2021) noted a slight trend indicating that a greater velocity-storage time constant was associated with increased overall motion-sickness sensitivity during fore-aft translational motion. Still, this correlation was weak and not statistically significant. Thus, their study did not provide strong evidence that the velocity storage time constant is a predictor of sensitivity to general motion sickness for fore-aft translation motion [Irmak et al., 2021]. In contrast, Dai et al. (2003) examined motion sickness during roll-head movements in vertical-axis rotation. They observed that as exposure duration increased, sickness decreased and subjects could tolerate more head movements. This was associated with a reduction of the velocity storage time constant, indicating a link between motion sickness and reduced velocity storage [Dai et al., 2003]. This suggests that the relevance of velocity storage may depend on the type of motion

stimulus.

Furthermore, research has shown that changes in postural control may precede motion sickness. Stoffregen and Smart (1998) demonstrated this in the moving-room paradigm, exposing standing participants to low-amplitude oscillatory visual motion that approximates the frequencies of natural postural sway. Although the visual motion was subtle, about half of the participants became motion sick, and those participants showed increased sway before reporting symptoms [Stoffregen and Smart, 1998]. Stoffregen et al. (2000) found a similar effect in a fixed-base flight simulator, in which seated participants were exposed to visually simulated roll motion, and those who later became sick exhibited greater head motion before symptom onset. These findings suggest that monitoring sway or head motion could help predict motion sickness [Stoffregen et al., 2000]. Postural training, such as balancing, vestibular exercises, or anticipatory movement strategies, can help improve postural control and, in turn, may reduce susceptibility to motion sickness. This is relevant for training astronauts and pilots, for example.

Keshner and Peterson (1995) proposed that head stabilization depends on three main mechanisms: voluntary motor control, reflexes, such as the vestibulocollic reflex (VCR) and cervicocollic reflex (CCR), and the passive mechanical properties of the head-neck system. The effectiveness of each mechanism depends on the frequency and plane of perturbation. Voluntary control functions best at low frequencies, below 1 Hz, while the VCR and CCR dominate between 1-2 Hz [Keshner and Peterson, 1995]. The VCR originates from the vestibular input and helps stabilize the head in space, while the CCR is based on neck proprioception and stabilizes the head relative to the trunk. Together, they compensate for unexpected body rotations. At frequencies exceeding these, the effects of mechanical resonance become visible. This can lead to head movement exceeding the resonance of the trunk, particularly in the horizontal (yaw) plane [Keshner et al., 1995].

Mirakhorlo et al. (2022) investigated how different sitting positions and vehicle seat configurations influence passenger motion comfort and the transmission of vibrations to the human body. They hypothesized that a low backrest improves trunk and head stabilization, whereas a high or full backrest constrains the spine and limits coordinated stabilization strategies. It was assumed that the low backrest allows stabilization of the trunk and head. The higher the backrest, the more it constrains lumbar and spine motion, thereby preventing a coordinated full-spine stabilization strategy and resulting in amplified head rotation [Mirakhorlo et al., 2022]. During the experiment, participants sat in various driving positions and were subjected to fore-and-aft, lateral and vertical vibrations with a wide bandwidth spectrum instead of considering the total body sway in the time domain, the authors analyzed the body response with transmissibility in the frequency domain by calculating transfer functions between the input signal (i.e. motion of the platform) and the measured signals of the pelvis, trunk and head motion. In this way, they were able to determine which specific frequency ranges were amplified, for example, by the body. This way, frequency-specific transmissibility analysis is used instead of traditional sway measurement methods to analyze motion response, as frequency-domain analysis allows evaluation of dynamic postural behavior (i.e., the body's response to oscillations at various frequencies). Sway measures in turn typically describe static or quasi-static postural behavior with global measures such as the movement of the center of pressure of the entire body or of individual joints. An additional advantage of frequency-domain analysis is that body responses and vibration excitation directions can be considered separately. In their study, Mirakhorlo et al. therefore examined the effect of low, medium, and high backrests on fore-and-aft, lateral, and vertical body translation and response, such as pitch, roll, and yaw. A low backrest was associated with reduced vibration transmissibility to the head, as it allows more freedom for active spinal stabilization. On the other hand, the respondents also rated the lowest backrest as the least comfortable. Furthermore, it was shown that a head-down posture, i.e., the posture seen during smartphone use, led to an additional increase in head movement. In addition, it was shown that visual input was significant for body stabilization at low frequencies. With eyes closed, there was an increase in head rotations [Mirakhorlo et al., 2022].

Kotian et al. (2025) conducted research to design a Motion Cueing Algorithm (MCA) using Model Predictive Control (MPC) that replicates specific forces from a real vehicle drive in a driving simulator, while intentionally minimizing motion sickness. This was done by exposing participants to a controlled dynamic movement in the Delft Advanced Vehicle Simulator (DAVSi). They found the configuration in which sickness reduction and the reproduction of the forces were balanced to be a good compromise.

Furthermore, they found that a configuration that focused only on reproducing the reference vehicle's specific forces resulted in the highest level of motion sickness [Kotian et al., 2025].

The use of simulator-based methods for motion sickness research is particularly interesting as they provide a more feasible and accessible testing environment than a real vehicle. Real-car motion sickness experiments often require a vehicle, a track or route, safety supervision, and multiple long exposures to induce motion sickness symptoms. Conversely, a driving simulator facilitates more straightforward control, repetition and manipulation of the motion stimulus while eliminating or mitigating practical constraints of the motion cueing experiment and traffic, weather, and other safety-related factors.

3

Problem Statement

3.1. Objectives

The objectives of this thesis consist of the following:

- Quantify individual postural sway under unperturbed conditions.
- Assess rotational motion perception under eyes-closed conditions and measure the individual velocity storage time constant.
- Assess dynamic head stabilization during dynamic motion in a driving simulator.
- Measure motion sickness during exposure to controlled vehicle motion in a driving simulator.
- Find the correlation between motion sickness and the individual perceptual and postural parameters.

3.2. Hypothesis

It is hypothesized that individuals with greater postural sway, reduced dynamic head stabilization, and a larger velocity storage time constant exhibit higher levels of motion sickness symptoms.

4

Methodology

The method proposed in this study was designed to quantify inter-individual differences in rotational motion perception and postural control and to relate these measures to subjective motion sickness susceptibility during controlled motion exposure. The experimental design was based on established experiments from the literature. The overall design, the participants, and various measurement methods and experimental descriptions are discussed below.

4.1. Overall design

A within-subject experiment was designed, in which all participants completed the same sequence of tests under controlled conditions. A motion sickness exposure test was employed at the end to minimize the carry-over effects of motion sickness symptoms on other performances. A repetition of the sway experiment after the motion sickness exposure was used to investigate the impact of motion sickness exposure on individual sway performance, thereby helping to identify the interaction between sway and motion sickness. The primary variables analyzed during the experiments were postural sway characteristics, dynamic head-neck stabilization metrics, the perceived rotational velocity, and motion sickness severity. The experiment lasted approximately 2 hours.

4.2. Participants

A total of 22 healthy adult participants (6 female, 16 male) were recruited from the student population at the Technical University of Delft and through personal networks. The participants were aged 18-34, with an average age of 22 years, and heights ranging from 165 to 194 cm, with an average of 178.55 cm, as shown in Figure 4.1 and Figure 4.2, respectively. Individuals with known medical impairments, postural stability issues, or vestibular disorders were excluded from the experiment. Before participation, all participants were provided with the 'Participation Information and Informed Consent' form, approved by the Human Research Ethics Committee (HREC) (ID 4819) of the Technical University of Delft. This form contains detailed information about the experimental protocol, informs them of their potential risks, and the mitigation actions taken. All participants were informed that they could withdraw at any time without providing a reason. The form was signed by both the participant and the responsible researcher.

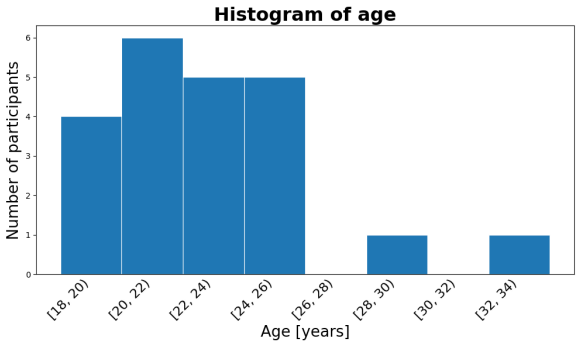

Figure 4.1: Frequency distribution of age

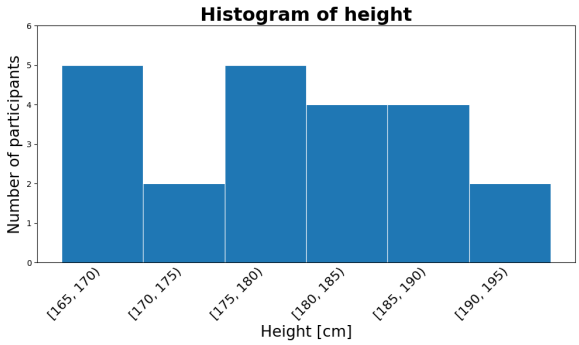

Figure 4.2: Frequency distribution of height

4.3. MSSQ

Before participants began the physical experiments, they completed the Motion Sickness Susceptibility Questionnaire (MSSQ), as presented in Section C.1. This questionnaire was used to estimate an individual's susceptibility to motion sickness and identify the motion most effective in causing it. The questionnaire begins with several background questions, including age, sex, height, and weight, and asks their medical impairments and susceptibility to motion sickness. This is followed by two sections: the first part concerns travel experience and MS, before the age of 12. The second part concerns the experience of travel and motion sickness over the past decade. The questionnaire provides a general overview of an individual's experience and susceptibility to motion sickness throughout their life. Following Golding's (1998) scoring method, a higher score indicates higher susceptibility [Golding, 1998]. This scoring method is discussed in more detail in Section 5.5.

4.4. Standing postural sway

Postural sway was first measured in the standing position under two conditions: eyes open (EO) and eyes closed (EC), with no additional disturbances. For comparability, each subject underwent the same procedure: standing upright on a rigid surface, adopting a standardized position with the feet spaced about a hip's distance apart and the arms along the sides. The subjects were told to hold their heads upright. According to Luo et al. (2018), each trial lasted 90 seconds, with a 1-minute rest between trials [Luo et al., 2018].

The sway was measured using a headband with a Movella XSENS DOT IMU. This sensor uses three physical sensing elements: a tri-axial gyroscope, a tri-axial accelerometer, and a tri-axial magnetometer (compass). The gyroscope measures the angular velocities with a range of ±2000°/s, the accelerometer measures the linear acceleration with a range of ±16g, and the magnetometer measures the Earth's magnetic field in order to offer heading reference [Xsens Technologies B.V., 2020]. By combining these, the sensor can provide full 3D tracking in all three axes. The gyroscope and accelerometer sample rates are 800 Hz. However, instead of communicating the raw sensor signals, the Movella DOT uses a strapdown integration (SDI) algorithm to reduce the rate to 60 Hz while preserving accuracy. The result is then fed into Movella's sensor fusion algorithm (XKFCore), a Kalman filter-based proprietary algorithm that fuses the three sensor modalities (gyroscope, accelerometer, and magnetometer) to provide drift-free orientation estimates. Orientation is provided as quaternions or as Euler angles (roll, pitch, and yaw) and communicated wirelessly via Bluetooth to the receiving device at 60 Hz [Xsens Technologies B.V., 2020]. To estimate head orientation free from drift and to measure sway for the participants in this study, processed orientation outputs rather than the raw inertial sensor data were used.

4.5. Sitting postural sway

Following the standing sway test, a seated sway test was included to enhance validity in the context of automated vehicles, as this better simulates the passenger environment. To conduct this test, the participant was seated in the rotational seat, shown in Figure 4.3, and the previous two conditions

(EO & EC) were repeated. Again, the sway was measured using the XSENS head sensor. To ensure comparability, all participants received the same instructions: sit straight with the knees at almost 90 degrees, keep the head upright without touching the headrest, and keep the hands on the thighs. They were asked to focus on stabilizing their head. Each trial lasted for 90 seconds, with a 1-minute break between trials. It was visually confirmed that participants contacted the full seat back, but not the headrest.

4.6. Dynamic postural stabilization test

The dynamic stabilization test used the DAVSi to replicate Mirakhorlo's (2022) experiment and evaluate head motion during whole-body vibration. Participants were sequentially exposed to fore-aft, lateral, and vertical wide-band random noise signals (0.1–12 Hz) with a motion amplitude of 0.3 m/s^2 rms. Each directional excitation lasted for 60 seconds and included a 3-second fade-in/out period to prevent abrupt movement, giving a total trial duration of approximately 200 seconds [Mirakhorlo et al., 2022]. To measure movement, one XSENS sensor was placed on the head using the headband, while the second was placed on the seat. Participants were instructed to look forward without using the headrest and stabilize their head during the movement.

Figure 4.3: Rotational Seat

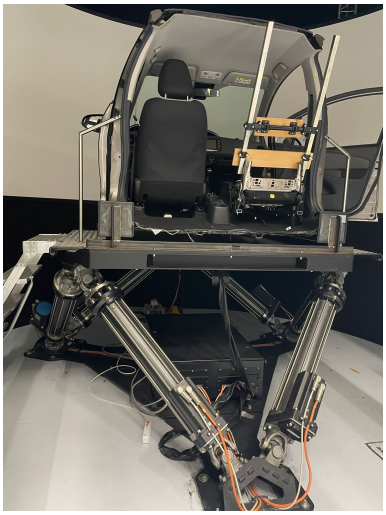

Figure 4.4: DAVSi

4.7. Motion perception experiment

The rotational perception test assessed how the participant perceives self-motion during yaw rotations while blindfolded. To do this, the EVAR paradigm described in Chapter 2 was employed. Based on the experiment by Bertolini et al. (2011), the test consisted of four trials of yaw rotation, two in the counterclockwise direction and two in the clockwise direction, following the right-hand rule. By limiting the number of rotation trials, the effects of decreasing alertness were avoided. To produce rotational motion, a motorized rotational chair capable of controlled yaw rotation was used, shown in Figure 4.3. The seat was adjusted such that the participant's vestibular organs were positioned as close as possible above the axis of rotation. By minimizing the distance between the vestibular organs and the axis of rotation, linear acceleration was minimized, and the possibility of motion sickness was reduced. Participants were securely seated and instructed to maintain an upright posture with the head against the headrest throughout all four trials.

Following Bertolini et al. (2011), each trial consisted of a constant rotation rate of 90°/s for 90 seconds, with accelerations and decelerations of 90°/s^2. A post-rotatory recording was made until the participant reported no further perception of rotation. Participants were asked to report their sense of rotation using a lever with their dominant hand. This was used to measure their velocity storage time constants. To avoid sensory input, such as motor noise and light from the windows, the participant was blindfolded and wore headphones that delivered brown noise. Between each trial, a 30-second break was provided,

during which the participant removed the blindfold and headphones [Bertolini et al., 2011]. A participant positioned in the correct experimental set-up is shown in Figure A.1.

To measure actual motion and perceived motion during yaw rotation, a hand lever and two XSENS sensors, one on the head and one on the seat were used, which are shown in Figure 4.5 and Figure 4.6, respectively; participants were instructed to continuously indicate their perceived rotation velocity by moving the lever in the direction of the perceived rotation. The angle of the lever corresponds to the perceived rotational velocity, and returning the lever to the neutral position indicates no perceived motion. This measurement allows to investigate whether angular velocity was perceived as constant, increasing, or decreasing. However, only the relative magnitude can be measured, and this does not allow estimation of the actual magnitude of the perceived angular velocity [Bertolini et al., 2011].

Figure 4.5: Joystick in (right) hand

Figure 4.6: IMU XSENS Sensor, with and without headband

4.8. Motion sickness exposure test

For the Motion Sickness Exposure Test, an MPC-based motion cueing algorithm with a sensory conflict weight of zero from Kotian et al. (2025) was used. This algorithm achieves high fidelity and shows high levels of experienced motion sickness. The driving scenario consisted of 240-second laps, followed by a 10-second break, repeated 6 times. The scenario was urban driving with vehicle speeds ranging from 0 to 70 km/h and stop-and-go sequences, including traffic lights and crossing pedestrians. To follow the procedure from Kotian et al., the subject's motion sickness level was surveyed every 30 seconds, prompted by an auditory beep through the headphones. The level of sickness was determined using the MISC (Misery Scale), of which the levels and corresponding symptoms are shown in Table E.1. The test was stopped immediately when the MISC reached a score of 6, which equals slight nausea [Kotian et al., 2025].

4.9. Repetition of sway test

Both the standing and sitting tests were repeated after the motion sickness exposure test to investigate the influence of MS symptoms on postural sway. First, the standing test was performed with eyes open, then with eyes closed. Next, the same conditions (EO & EC) were performed in the sitting condition. The sway was again measured using the XSENS sensor on the head.

4.10. MSAQ

The experiment ended with completing the Motion Sickness Assessment Questionnaire (MSAQ), a 16-item questionnaire composed of 4 subcomponents that assessed various types of motion sickness. The question items and the scoring method for this questionnaire are presented in more detail in Section 5.5.

5 Analysis

5.1. Sway

Based on the analysis of Luo et al. (2018), the sway is analyzed using seven metrics following Luo et al. (2018), derived from the IMU data: standard deviation (SD) from the anteroposterior (AP) and mediolateral (ML) head rotation angle, mean rotation velocity (MV) from the anteroposterior and mediolateral, and the fuzzy approximate entropy (fApEn) from anteroposterior and mediolateral head rotation angle, and the total path length (TPL) [Luo et al., 2018].

Before calculating these sway metrics, the raw signals were preprocessed. After transforming the quaternion outputs from the XSENS sensor to relative Euler angles (pitch as *AP* and roll as *ML*), the first 5 s from each trial were removed to discard the initial stabilization phase, resulting in $\sim$85 s of data per trial. After that, the signals were passed through a zero-phase Butterworth band-pass filter comprised of a 2nd-order 0.1 Hz high pass to remove slow sensor drift, and a 4th order 20 Hz low pass to remove high-frequency noise, and therefore, keep the postural sway frequency band (0.1 to 3 Hz). SD, MV, and TPL were calculated on the filtered signals at 60 Hz. In case of fApEn, the signals were first downsampled to 20 Hz, taking each third sample, as in Luo et al. (2018) [Luo et al., 2018].

SD_AP and SD_ML are calculated using Equation 5.1 and Equation 5.2, respectively, where T (= 1/f_s) is the sampling interval and f_s is the sampling frequency equal to 60 Hz in this case. AP_i and ML_i are the angular displacement time series in the respective directions, N is the data length, and μ_{AP} and μ_{ML} are the mean values of AP_i and ML_i. The MV in the AP and ML directions is calculated using Equation 5.3 and Equation 5.4. TPL is the total Euclidean distance of the 2D angular sway trajectory, calculated by combining the AP and ML directions into one measure, as shown in Equation 5.5.

$$SD_{AP} = \sqrt{\frac{1}{N}\sum_{i}^{N}|AP_i - \mu_{AP}|^2} \tag{5.1}$$

$$SD_{ML} = \sqrt{\frac{1}{N}\sum_{i}^{N}|ML_i - \mu_{ML}|^2} \tag{5.2}$$

$$MV_{AP} = \frac{1}{N-1}\sum_{i=1}^{N-1}\frac{|AP_{i+1} - AP_i|}{T} \tag{5.3}$$

$$MV_{ML} = \frac{1}{N-1}\sum_{i=1}^{N-1}\frac{|ML_{i+1} - ML_i|}{T} \tag{5.4}$$

$$\text{TPL} = \sum_{i=1}^{N-1}\sqrt{(AP_{i+1} - AP_i)^2 + (ML_{i+1} - ML_i)^2} \tag{5.5}$$

Computing fApEn

Given a time series $\{u(i) : 1 \leq i \leq N\}$, $fApEn$ is computed by using the following steps:

1. **Template vectors:** A sequence of mean-centred template vectors of length m is constructed:

$$X_i^m = \{u(i), u(i+1), \ldots, u(i+m-1)\} - \frac{1}{m}\sum_{j=0}^{m-1} u(i+j), \quad i = 1, 2, \ldots, N-m+1 \tag{5.6}$$

2. **Chebyshev distance:** The maximum absolute difference between two template vectors X_i^m and X_j^m is computed:

$$d_{ij}^m = \max_{k\in[0,\,m-1]} \left| \left(u(i+k) - \frac{1}{m}\sum_{k=0}^{m-1} u(i+k) \right) - \left(u(j+k) - \frac{1}{m}\sum_{k=0}^{m-1} u(j+k) \right) \right| \tag{5.7}$$

3. **Fuzzy membership function:** The similarity between two vectors is quantified using an exponential fuzzy membership function:

$$D_{ij}^m(n,\, r) = \exp\left(-\left(\frac{d_{ij}^m}{r} \right)^n \right) \tag{5.8}$$

4. **Mean similarity φ^m:** All pairwise similarities are averaged:

$$\varphi^m(N,\, r) = \frac{1}{N-m+1} \sum_{i=1}^{N-m+1} \ln \left(\frac{1}{N-m+1} \sum_{\substack{j=1 \\ j\neq i}}^{N-m+1} D_{ij}^m \right) \tag{5.9}$$

5. **fApEn:** Finally, fApEn is defined as the difference between φ^m and φ^{m+1}:

$$fApEn(m,\, n,\, r) = \varphi^m(n,\, r) - \varphi^{m+1}(n,\, r) \tag{5.10}$$

The parameters were set to $m = 2$, $n = 2$, and $r = 0.2 \times \sigma$, where σ is the standard deviation of the downsampled signal, following Luo et al. Prior to computing fApEn, the signal was downsampled from 60 Hz to 20 Hz, as the physiologically relevant bandwidth of postural sway is 0–10 Hz and oversampling introduces artificial colinearities [Luo et al., 2018].

For each outcome, a three-factor repeated-measures ANOVA was used, with time point (*before & after MS exposure*) crossed with postural (*Stan & Sit*) and visual (*EO & EC*) condition. Before performing any paired comparisons, the Shapiro-Wilk test was used to assess the normality of the difference scores. The outcomes with at least one condition that was non-normal were analyzed using the Wilcoxon signed-rank test. A paired t-test was performed for the normally distributed outcomes. Effect sizes were reported as Cohen's d (parametric) or rank-biserial r (non-parametric).

5.1.1. Correlation between sway metrics

A Spearman correlation matrix between the sway and dynamic stabilization metrics was computed after averaging all conditions (*Stan EO, Stan EC, Sit EO, Sit EC*) and timepoints (*before & after MS exposure*) for all participants. The results are shown in Figure A.36, which indicates that some sway metrics have a significant positive correlation with the stabilization metrics. SD_AP and SD_ML of sway both show significant correlation with SD_AP and the Mean Displacement of dynamic stabilization.

Next, a Bonferroni correction was applied: 19 variables were included in the correlation matrix, 171 unique pairwise correlations were tested, and thus a Bonferroni-corrected significance threshold of α = 0.05/171 = 0.00029 was used. This correction was applied to reduce the likelihood of a Type 1 error arising from the large number of simultaneous comparisons. The outcome is shown in Figure 5.1.

The sway metrics showed strong correlations with one another. The z-scores, determined by standardizing each of the five sway magnitude metrics (SD_AP, SD_ML, MV_AP, MV_ML, and TPL) across participants and averaging the resulting z-scores into a single composite index per participant, also showed very strong correlations with the individual magnitude measures.

Secondly, the two complexity measures (fApEn_AP and fApEn_ML) were positively correlated with each other (ρ = 0.67) and were strongly negatively correlated with the magnitude measures (SD_ML and fApEn_AP: ρ = −0.84, p_$bonf$ $<$ 0.001; SD_AP and fApEn_AP: ρ = −0.74, p_$bonf$ $<$ 0.01). This shows that the greater the sway magnitude, the lower the neuromuscular complexity of postural control, as also discussed by Luo et al., suggesting the use of both magnitude and complexity measures in the present study [Luo et al., 2018].

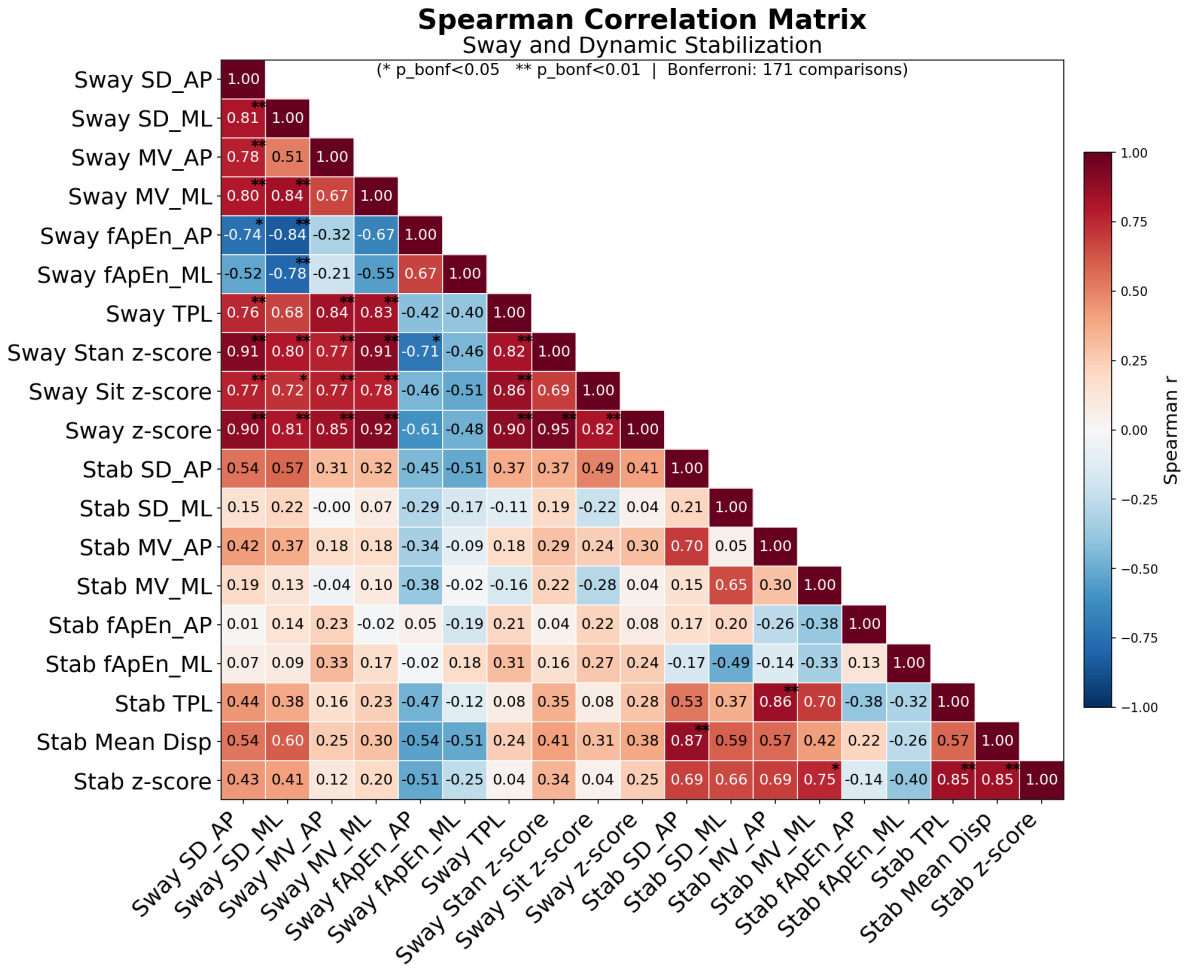

Figure 5.1: Spearman correlation matrix between the postural sway and dynamic stabilization metrics, averaged across all conditions (*Stan EO, Stan EC, Sit EO, Sit EC*) and timepoints (*before & after MS exposure*) for all participants Bonferroni correction (α = 0.05/171 $\approx$ 0.00029), * p_{bonf} <0.05, ** p_{bonf} <0.01

5.1.2. Effect of height

To check whether height affects sway, the seven metrics of sway in the standing condition are averaged across all time points and EO & EC conditions. For standing, the correlation between TPL and the height is shown in Figure 5.2. The correlations in the sitting condition are also determined, and the results per metric, both standing and sitting conditions, can be found in Table B.1. Based on the Spearman correlation coefficients, there is no meaningful correlation between height and sway in either standing or sitting conditions.

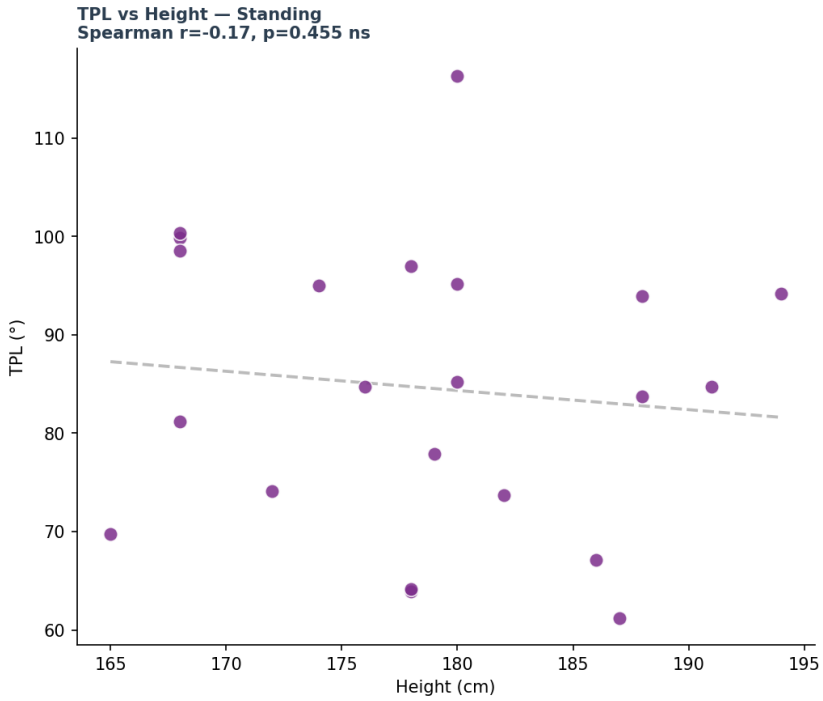

Figure 5.2: Correlation between TPL of sway and height

5.1.3. Individual sway

To analyze individual sway, each outcome *(SD_AP, SD_ML, MV_AP, MV_ML, TPL*) was z-scored and averaged across all conditions (*Stan EO, Stan EC, Sit EO, Sit EC*) and timepoints (*before & after MS exposure*). The z-score was used to combine the sway measures into a single dimensionless, composite index, allowing comparison among all individuals on a common scale despite the units and orders-of-magnitude differences among these measures. Figure 5.5 shows these results: the red bars indicate positive values (above-average sway), and the blue bars indicate negative values (below-average sway). From this, it can be seen that P04 is the most stable participant, consistently having low sway across all conditions, with a sway index of -1.55, while P10 stands out as an extreme outlier with a sway index of +2.11.

Figure 5.3 and Figure 5.4 show the z-score of each participant with the before and after motion sickness exposure, respectively. Here it also shows that P10 has acceptable sway *before* motion sickness exposure, but has unusually high (> 2·SD) sway *after* motion sickness exposure. This is most likely due to an error during measurement.

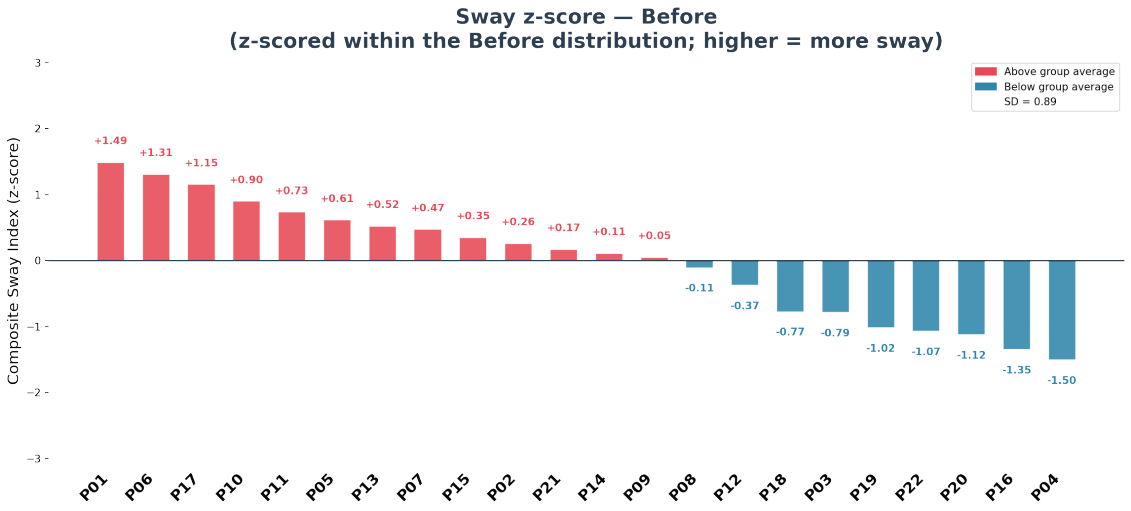

Figure 5.3: Z-score *before* conditions

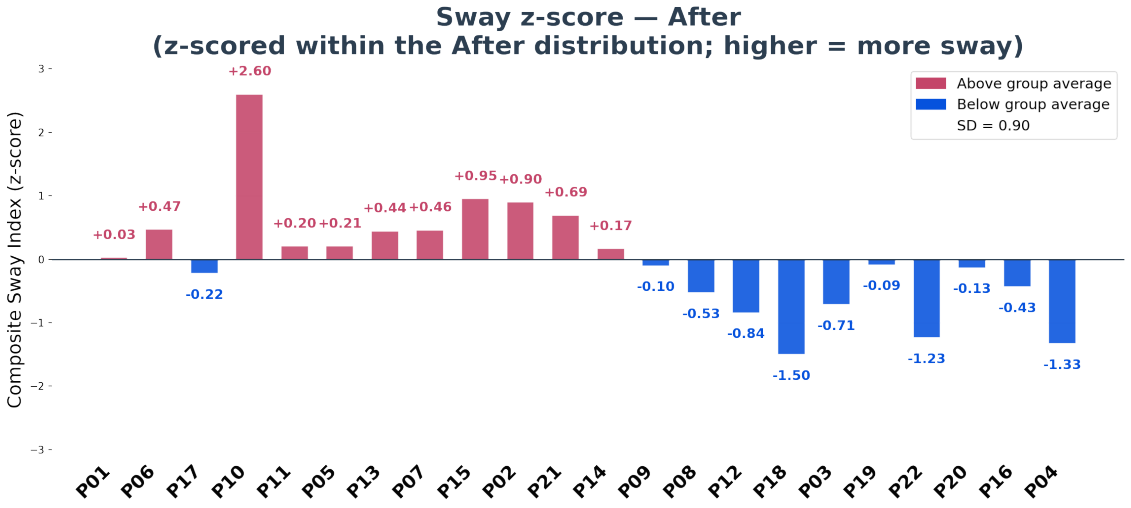

Figure 5.4: Z-score *after* conditions

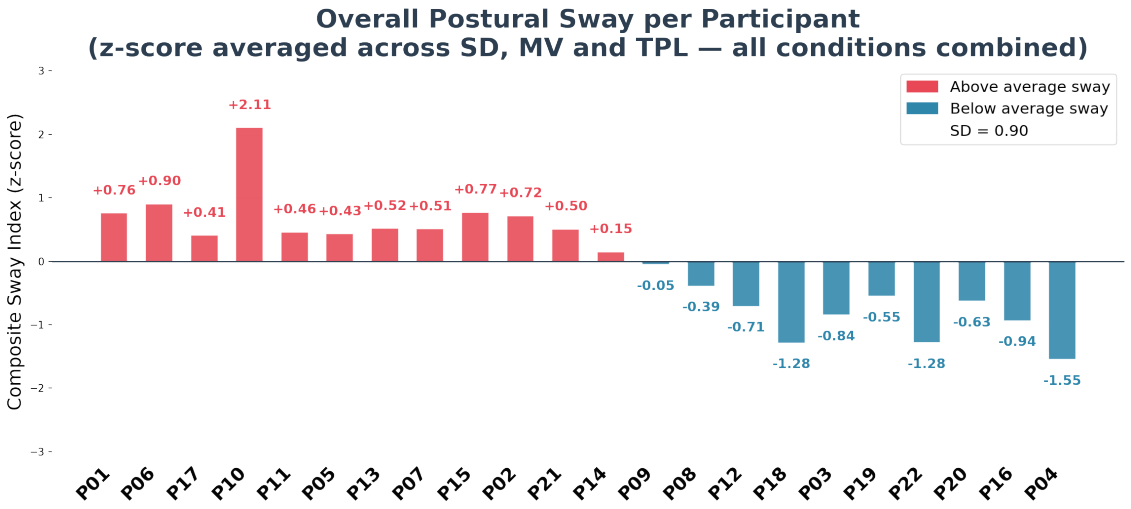

Figure 5.5: Overall postural sway per participant

5.1.4. Standing vs. sitting

Figure 5.6 shows the group means, with *before* and *after* conditions averaged together, for each outcome measure across the four conditions: Stan EO, Stan EC, Sit EO, Sit EC. It can be seen that, for all measures except fApEn_AP, the standing conditions have higher values than the sitting conditions. When comparing Stan EC and Stan EO, the eyes-closed condition shows greater sway amplitude and velocity. This is consistent with the expected effect of removing visual feedback. In contrast, the two sitting conditions show minimal differences, suggesting that visual feedback contributes less to balance control in the seated position.

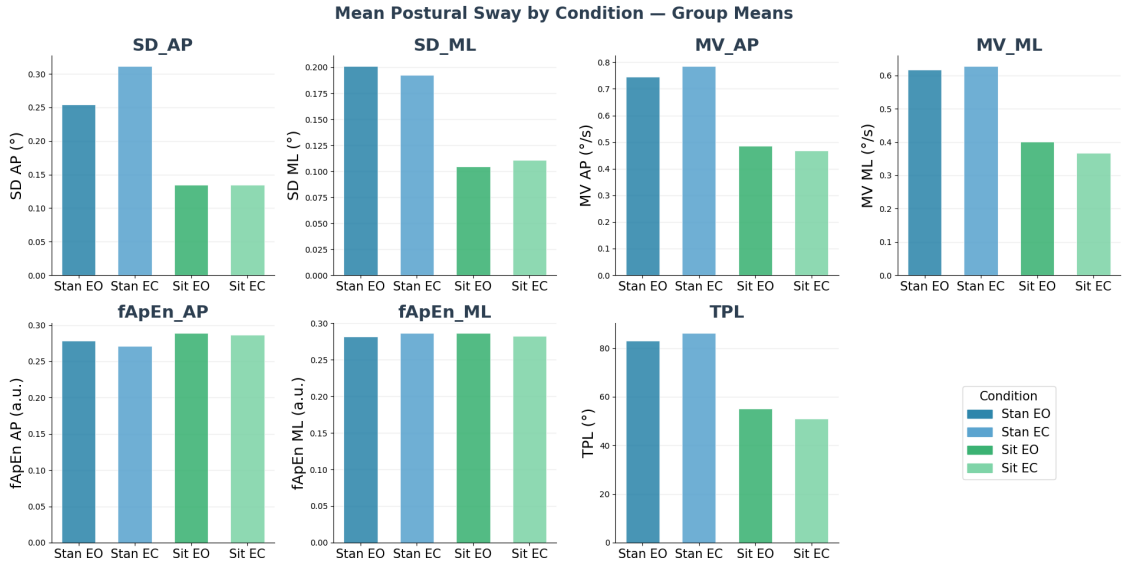

Figure 5.6: Group means of postural sway by condition

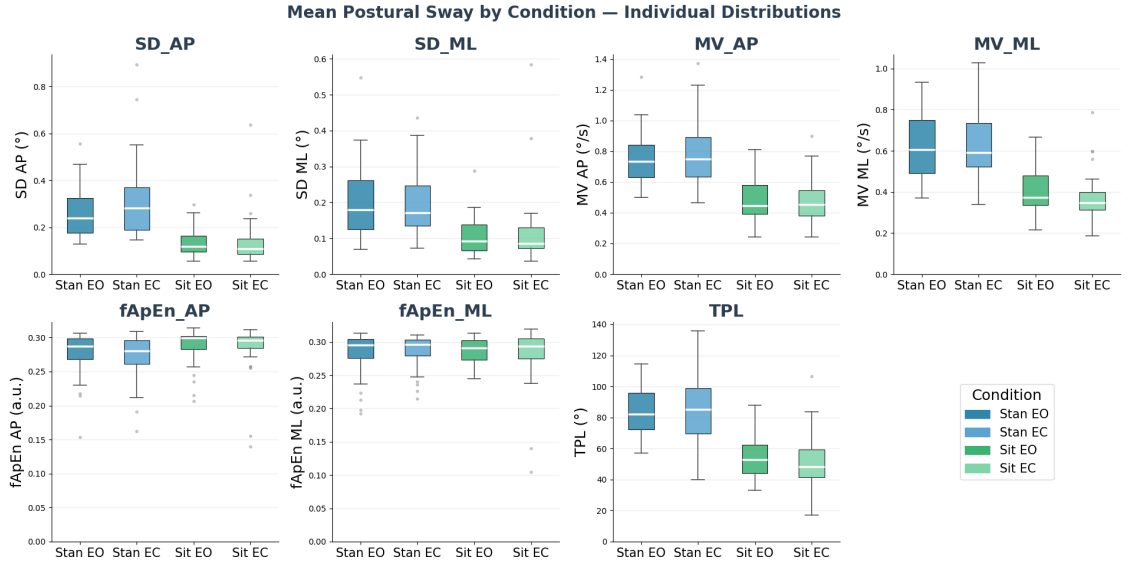

Figure 5.7: Box plot of sway by condition, with the median (center line), interquartile range (box edges), and 1.5×IQR whiskers; dots beyond whiskers are individual outliers

To investigate whether the large spread in the standing conditions, shown in Figure 5.7, reflects true inter-variability, the coefficient of variation (*CV = SD/Mean*) was calculated for each metric and each condition, averaged over the before and after timepoints. The results are shown in Table B.5 and

Table B.6 for standing and sitting, respectively. This indicates whether participants were actually more variable in standing than in sitting. However, the ratios are generally comparable across conditions.

The higher fApEn_AP values observed in the sitting conditions, shown in Figure 5.6, can be explained by the idea that the neuromuscular system produces more variable and adaptive movement patterns when postural demands are low. Standing, however, imposes greater constraints on balance, leading to more repetitive, stereotyped corrections that reduce the complexity of the signal [Luo et al., 2018].

5.1.5. Before vs. after motion sickness exposure

The effect of motion sickness exposure on postural sway is shown in Figure 5.8 and Figure 5.9 for the standing and sitting conditions, respectively. The motion sickness exposure test clearly affects the standing conditions, while no effect was detected in the sitting conditions.

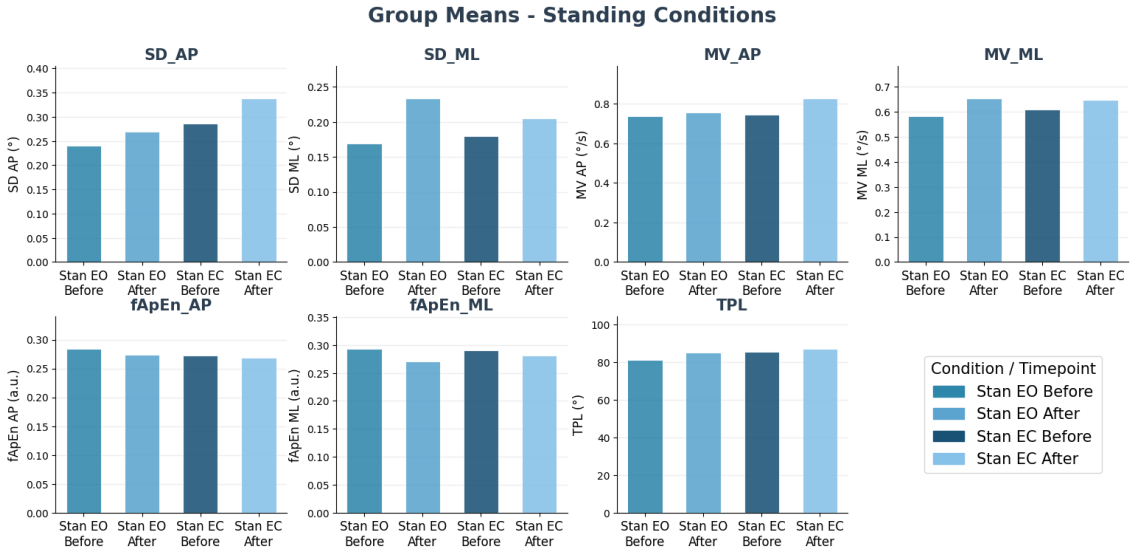

Figure 5.8: Group means of the standing sway conditions, both before and after motion sickness exposure.

Figure 5.9: Group means of the sitting sway conditions, both before and after motion sickness exposure.

The effect in the Stan EO condition was more clearly seen in the medial-lateral direction, namely SD_ML (+37.6%, p = 0.009, r = -0.62), indicating more medial-lateral sway displacement, MV_ML (+12.2%, p

= 0.034, d = 0.48), which implies greater change of the displacement in the medial-lateral direction. Furthermore, changes are seen in fApEn_AP (−3.5%, p = 0.036, r = 0.51) and fApEn_ML (−7.6%, p = 0.005, r = 0.68), both indicating less complex neuromuscular control after exposure.

Though there were no significant changes in the Stan EC condition, all measures increased in the expected direction (SD_AP +18.3%, SD_ML +13.8%, MV_AP +11.0%, MV_ML +6.5%). Given the small sample size (N = 22), these findings should be treated with caution. Specifically, a failure to obtain a statistically significant result does not necessarily mean that no such effect exists; a larger sample may be needed to demonstrate one.

There were no significant differences in postural sway in either of the sitting postures (Sit EO or Sit EC). Effect sizes for these measures were small to negligible, indicating no intervention-related change in postural sway in seated conditions.

Figure 5.10 presents the average After/Before ratio for each sway outcome across the four conditions. A value of 1 (indicated by the dashed line) means sway did not change after the motion sickness exposure, a ratio of >1 indicates sway increased, and a ratio of <1 means sway decreased after motion sickness exposure. For each condition and metric, Table B.3 shows the mean and SD for the ratio and the outcome of significance testing, including the p-value.

As mentioned in Subsection 5.1.3, P10 shows unusual high sway index after MS exposure, likely due to a measurement error. Therefore, the before-to-after analysis was repeated, excluding P10. These outcomes are presented in Table B.4. The effect is mostly minimal, as *SD_ML Stan EO* and *MV_ML Stan EO* still show a significant increase after MS exposure.

A Bonferroni correction was applied to account for the multiple comparisons with 28 outcomes (7 metrics x 4 conditions). The Bonferroni corrections equaled $0.05/28 = 0.00179$. The results are also shown in Table B.3 and Table B.4. None of the tests is significant under the Bonferroni correction.

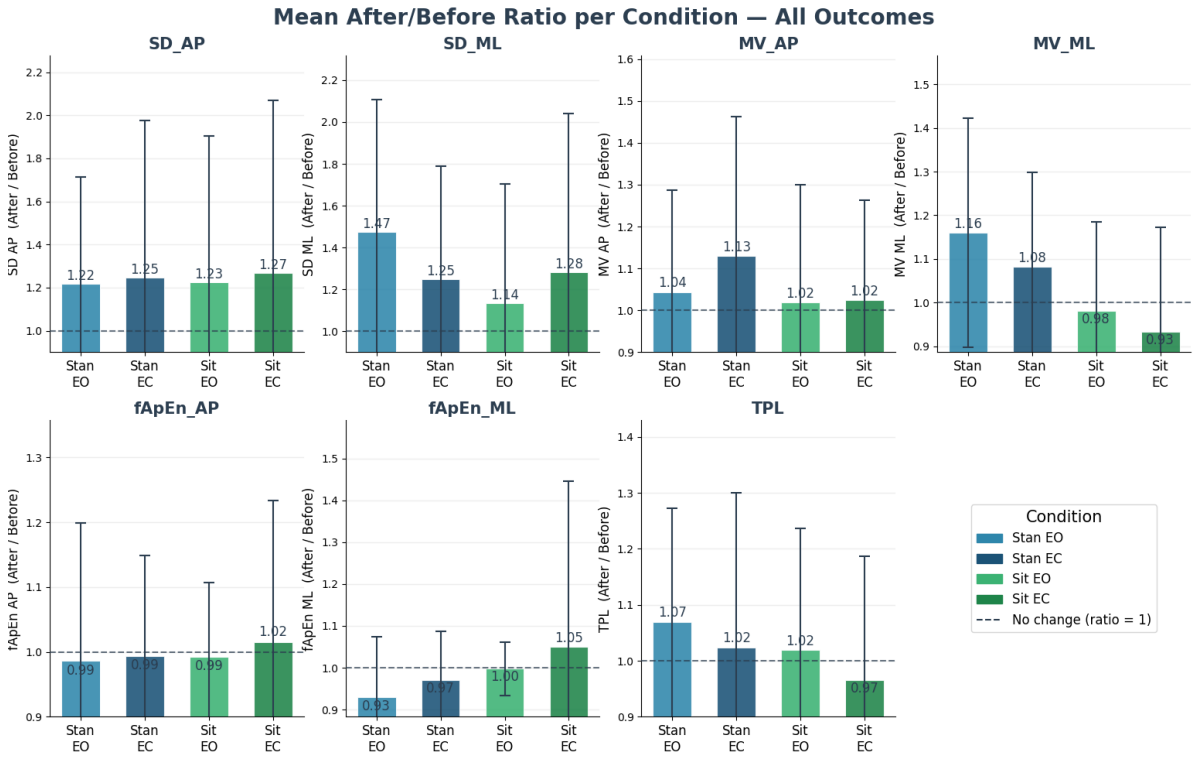

Figure 5.10: Mean ratio of after/before sway per condition,
where the dashed horizontal line indicates a ratio of 1, and the error bars represent variability across participants

To summarize the sway response across all five magnitude metrics, a composite ratio was computed

by averaging the After/Before ratio of SD_AP, SD_ML, MV_AP, MV_ML, and TPL for each participant, separately for all conditions combined, in standing only (Stan EO + Stan EC), and in sitting only (Sit EO + Sit EC). Across 22 participants, the standing composite showed a significant increase (mean = 1.150, p = 0.0143), and the combined composite also reached significance before correction (mean = 1.106, p = 0.0438), while the sitting-only composite showed no significant change (mean = 1.066, p = 0.3880). Excluding P10, the standing-only effect remained significant (mean = 1.131, p = 0.0284), whereas the combined effect no longer reached significance (mean = 1.079, p = 0.0837), and sitting are unaffected. These composite results are included in Table B.3 and Table B.4.

Overall, results suggest that exposure to motion sickness increased sway in the Stan EO. There was greater SD_ML (mean ratio = 1.473, p = 0.0021) and MV_ML (mean ratio = 1.160, p = 0.0094) after exposure to motion sickness in Stan EO, confirming greater and faster sway in the Medial-Lateral direction. A decrease was also observed in fApEn_ML (mean ratio = 0.929, p = 0.0.0327) in Stan EO after exposure, confirming reduced neuromuscular complexity. No significant increase was found for the other conditions, as their ratios were close to 1.0 across all outcomes.

5.2. Dynamic postural stabilization

To assess dynamic postural stabilization, head movement, specifically rotation and not translation, was analyzed during the Mirakhorlo motion experiment. Two sets of recordings (P01 & P21) are excluded due to errors in the measurement process. A band-pass filter from 0.1 to 12 Hz was applied to match the stimulus bandwidth. This 0.1 Hz lower cutoff frequency will exclude sensor noise and voluntary motion, whereas the 12 Hz upper cutoff frequency is sufficient to capture both the active stabilization response and the passive biomechanical head-seat coupling at higher frequencies. Since the motion induces a sequential perturbation in all three axes (X, Y, and Z), the rotation was evaluated across all perturbation directions.

For the analysis, the same seven metrics as sway, discussed in Section 5.1, were used, as well as the Mean Displacement (deg), which reflects the average angular distance of the head from its neutral position. The final results for each metric are presented in Table B.7. Figure 5.11a and Figure 5.11b present the Total Path Length and Mean Displacement of each participant during the Mirakhorlo motion in the driving simulator.

In general, participants demonstrated moderate head stabilization during the perturbation period. The total path length averaged across participants is 1676.48 $\pm$ 527.9 deg, while the averaged mean displacement is 0.96 ± 0.21 deg. Lower values indicate more effective head stabilization against perturbation. Inter-individual variability is observed across all parameters, suggesting that the dynamic stabilization strategy and performance differed between participants despite identical perturbation conditions.

Mean velocity in the AP direction (MV_AP: 6.12 $\pm$ 2.26 deg/s) was much higher than in the ML direction (MV_ML: 3.82 $\pm$ 0.95 deg/s), also seen in most of the participants. This is likely due to a greater available range of motion in the AP direction, resulting in larger and faster residual head movements in response to fore-aft perturbation forces. MV_AP also showed the most individual variability, suggesting that fore-aft head motion is attenuated to different degrees in each individual. Signal complexity, measured by fApEn, was similar across participants (SD of 0.017 in AP and 0.026 in ML). This suggests that the temporal pattern of the stabilization response was preserved across participants, despite substantial differences in velocity. These moderate fApEn values at the group level indicate a flexible, adaptive neuromuscular response to whole-body perturbation.

Figure 5.1 shows the Spearman correlation of the dynamic stabilization metrics with each other as well. They show a positive, moderate-to-strong correlation with each other. The composite z-score correlated strongly with all individual stabilization metrics. Noticeably, the correlations between sway and stabilization were weak and non-significant after Bonferroni correction. This suggests that these capture different aspects of postural behavior.

Furthermore, P11 can be identified as an outlier, using the criterion of mean $\pm$ 2*SD, for the metrics SD_AP, MV_AP, MV_ML, and TPL, displayed in Section A.2. These results suggest that head control in P11 was less successful, as indicated by greater residual head motion and angular velocity. P11 also

has the lowest fApEn value in the AP direction, indicating large-amplitude, low-complexity head motion. This suggests that a reactive, rather than an anticipatory, head-stabilization response was used during the Mirakhorlo perturbation.

On the other hand, P03 and P07 demonstrated the most effective head stabilization. P03 showed the lowest AP displacement and the lowest mean displacement, whereas P07 displayed the lowest total path length. In addition, both subjects have higher fApEn values, indicating better adaptation to the perturbation.

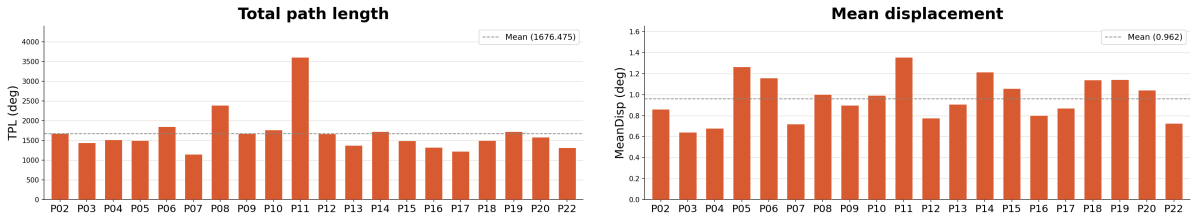

(a) Total Path Length of each participant during dynamic postural stabilization

(b) Mean Displacement of each participant during dynamic postural stabilization

Figure 5.11: TPL and Mean Displacement during dynamic postural stabilization

As in Subsection 5.1.3, a composite score for the dynamic stabilization measures was computed. The z-score for each magnitude (SD_AP, SD_ML, MV_AP, MV_ML, and TPL) was averaged for every subject, resulting in the following data presented in Figure 5.12. The red bars represent a greater-than-average magnitude, and the blue bars represent a below-average magnitude. P11 is an outlier once again, having a final composite z-score of +2.53. This value exceeds 2·SD, indicating poor stabilization during dynamic movement. P07, on the other hand, has the most negative composite z-score in the group (-0.9), indicating the most effective stabilization response across the group.

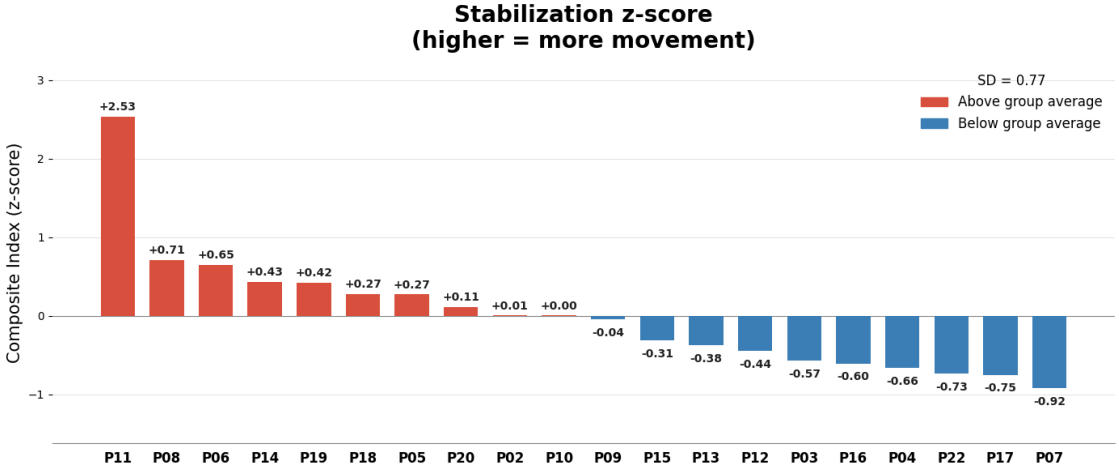

Figure 5.12: Composite index z-score dynamic postural stabilization

5.3. Motion perception

Figure 5.13 shows the angular velocity recorded by the XSENS sensor placed on the seat during the constant counterclockwise (CCW) rotation. The upper plot displays the body-frame angular velocity components over time. The yaw rate shows a step function with a consistent plateau of approximately 90 °/s, corresponding to the constant rotation phase. The pitch and roll rate remain close to zero, confirming that the motion is predominantly yaw rotation. After 90 seconds, the seat decelerates, causing the angular velocity to decay to zero. The lower plot on Figure 5.13 presents the cumulative yaw angle, which increases monotonically from 0° to approximately 8000° during the constant rotation phase.

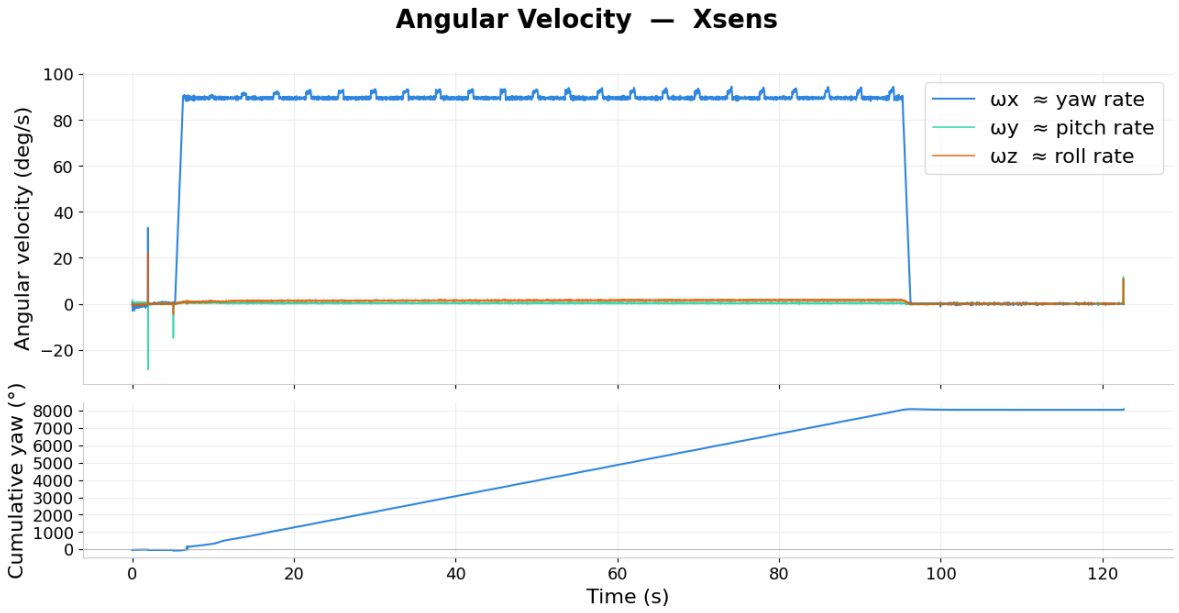

Figure 5.13: Example Angular Velocity of Rotational Seat with IMU

Figure 5.14 shows the angular velocity of the seat and the change of angle on the same plot. The data extracted from the joystick are shown as the red line and represent the participant's perceived rotational motion, plotted as the lever's angle change over time. This shows that the seat's deceleration is almost immediately perceived as a change in rotational direction. The angle's magnitude corresponds to the perceived velocity's intensity, while its sign indicates the direction of the perceived velocity: positive angles correspond to counterclockwise perceived movement, and negative angles correspond to perceived clockwise movement.

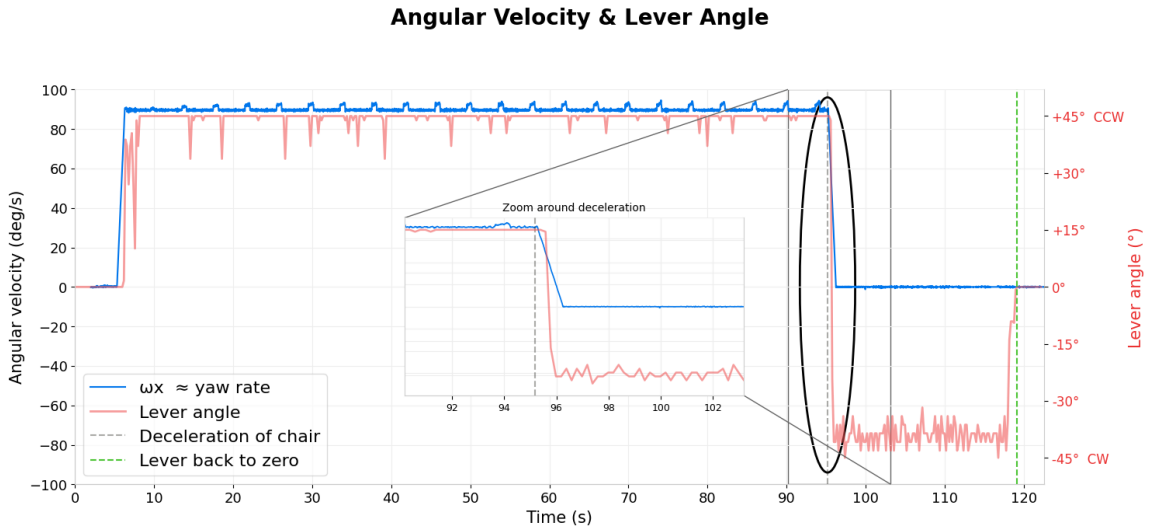

Figure 5.14: Example Angular Velocity and Lever on Same Graph, including zoom on deceleration of seat

Figure 5.14 also shows that during constant rotation from 0 to 90 seconds, the joystick remains at 45 degrees, which is the maximum, to the left. This indicates a constant perceived motion in the CCW direction. At 90 seconds, marked by the vertical red line, the rotation is stopped by a deceleration

of -90°/s^2. For all participants, the lever angle was immediately set to -45 degrees after deceleration, indicating a perceived rotation in the opposite direction despite the participant being stationary. In this case, the illusion of motion gradually decays to zero within approximately 24 seconds, indicated by the green dotted line. In this study, the time between the two vertical lines on Figure 5.14 represents the individual velocity storage time constant. Since the perceived rotational velocity was encoded as a lever angle, the lever's return to its neutral position is the most direct and unambiguous perceptual endpoint. Unlike Bertolini et al. (2011) and Irmak et al. (2021), who defined perceived velocity as the lever's spinning rate and derived the time constant from the 63.2% decay point.

For each participant, the individual velocity time constant is determined during each trial. The median over the four trials is used to compare the final results. These final values and their distribution are shown in Figure 5.15 and Figure 5.16, respectively. The average of the final scores is 21.34 seconds. A number of people reported a very short perceived rotation, while others felt like spinning for more than 5 minutes after deceleration.

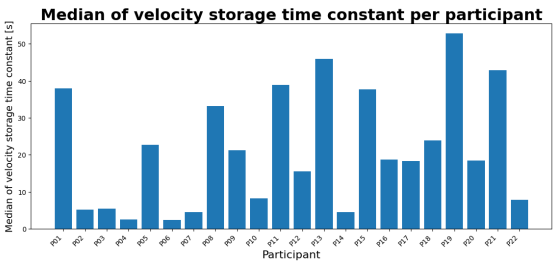

Figure 5.15: Median of velocity storage time constant per participant

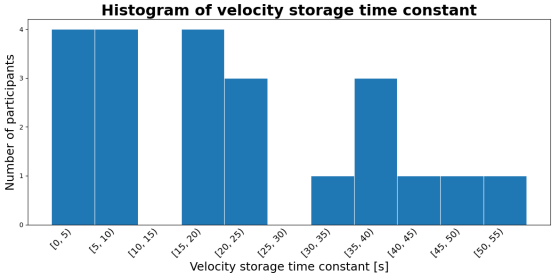

Figure 5.16: Frequency distribution of the median of the velocity storage constant

5.4. Motion sickness exposure

During the motion sickness exposure experiment, the sickness level was recorded every 30 seconds per trial. To compare the participants' sickness, both the average of their MISC scores across the six laps and their final MISC score are used. The development of motion sickness symptoms over time is shown in Figure 5.17. The thick blue line shows the mean MISC across all participants at each time point. It shows a clear increase, indicating that participants felt progressively sicker as the experiment progressed. The light blue band shows the interquartile range and widens over time. This indicates a spread between participants; some got sicker than others. The other lighter lines show the individual trajectories. The sawtooth pattern shows that the MISC scores drop at the start of each new run and then climb again. This shows the short recovery time between each trial. Since it does not fully return to baseline after each trial, this indicates that participants did not fully recover during the break. The vertical lines mark the boundaries between the 6 runs.

Figure 5.18a and Figure 5.18b show the results of the average of the MISC score during all six laps and the final value each participant reported, respectively. Two participants experienced a sickness level of 6 during the fifth trial and, therefore, did not complete the last trial. For those, '6' is used during every prompted MISC score for the last trial. Three participants, P03, P17 and P18, reported (almost) no symptoms. The subjects who indicated more severe symptoms than average are P01, P07, P11, P19, and P21.

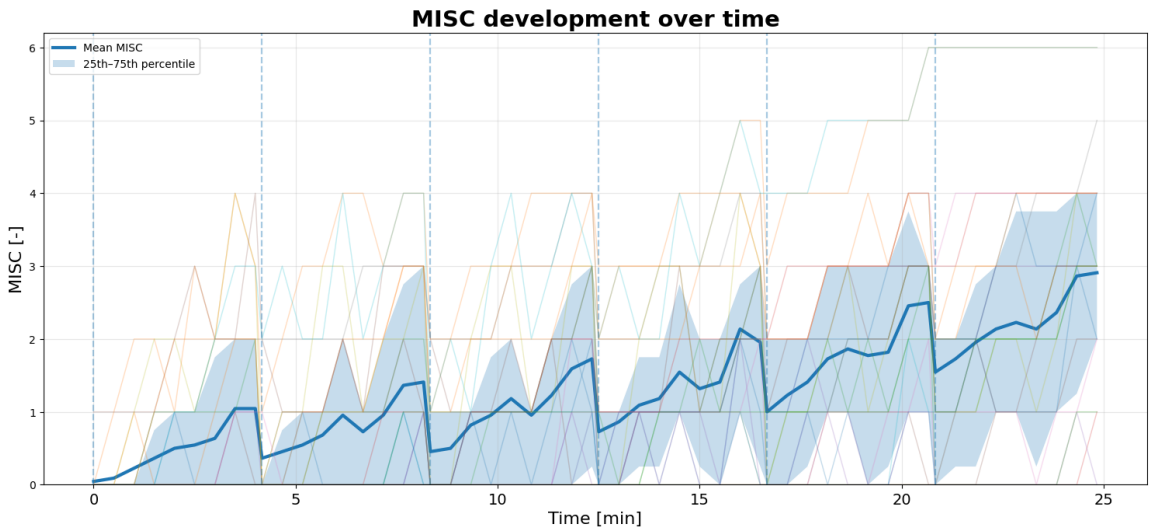

Figure 5.17: Development of motion sickness symptoms

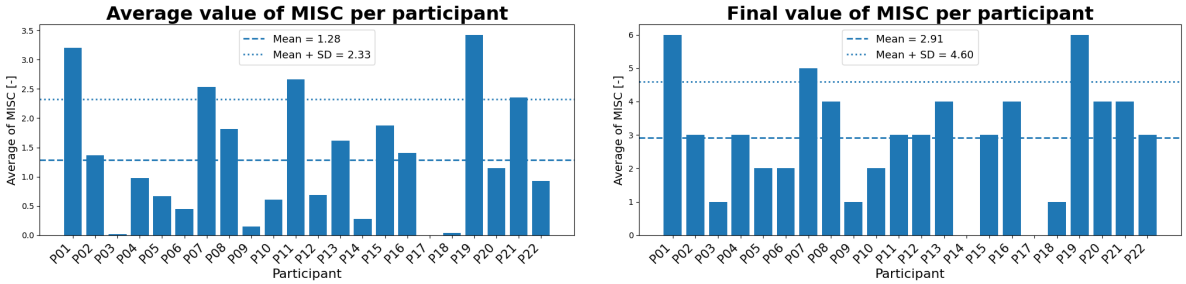

(a) Average of MISC per participant

(b) Final value of MISC per participant

Figure 5.18: MISC scores per participant

For the average score, the minimum is 0, the maximum is 3.43, and the average is 1.28. For the final values, the minimum is 0, the maximum is 6, and the average is 2.91. The distribution of the average and the final value are shown in Figure 5.19a and Figure 5.19b, respectively.

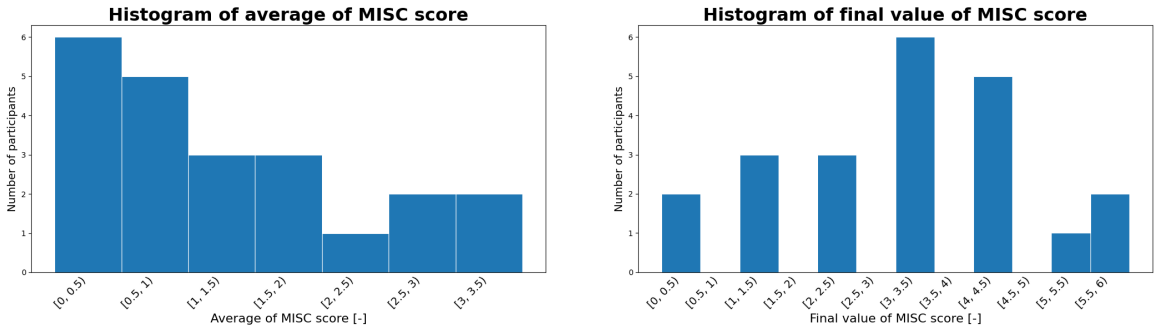

(a) Frequency distribution of average of MISC score

(b) Frequency distribution of the final value of MISC score

Figure 5.19: Frequency distributions of MISC scores

There was no significant effect found for sex in MS. The individual average and final MISC score are shown in Figure 5.20 for female (n=6) and male (n=16) participants. The horizontal lines indicate the

group means. It shows that females scored slightly higher on average, but the difference was not statistically significant (average MISC: t = 1.00, p = 0.37; final MISC: t = 0.37, p = 0.72). The small female sample size limits the power to detect a true difference.

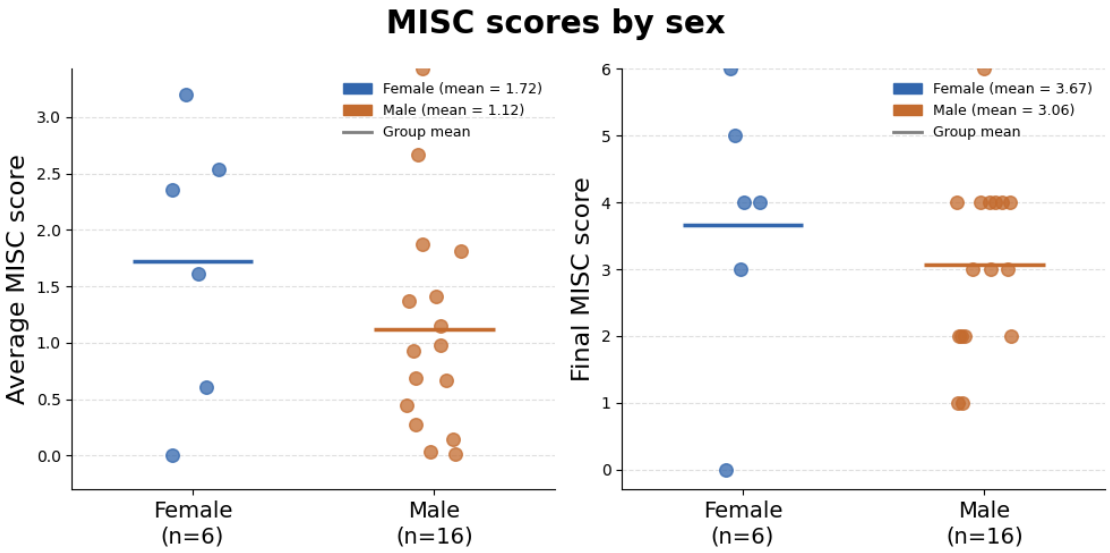

Figure 5.20: Average and final misc score per sex, including mean

5.5. Questionnaires

The scores for both questionnaires are calculated separately. The answers to the general/background questions are not graded specifically, but can be used for later background research. For the childhood and adult experience questions, Golding (1998) introduced a revised scoring method in which a higher score indicates greater susceptibility [Golding, 1998].

The scoring method is as follows: for both the childhood (A) and adult (B) experience separately, first sum the number of transportation types experienced at least once (i.e., a maximum of 9). Next, by using the scoring points shown in Table 5.1 and summing these for each mode of transport or motion, the total sickness score can be determined. Then, Equation 5.11 is used to determine the final score. The total MSSQ raw score is then calculated by summing the final values of both section A and section B, as shown in Equation 5.12.

The results of the MSSQ have a mean of 37.77 with a standard deviation of 32. The distribution of the results of the MSSQ is shown in Figure 5.21a. This shows that the subject group has a low-to-moderate average susceptibility, with wide individual variation. This is consistent with Golding (2006), who stressed that susceptibility to motion sickness varies greatly between individuals [Golding, 2006].

Table 5.1: MSSQ response scale and corresponding scoring values.

Never	Rarely	Sometimes	Frequently	Always
0	1	2	3	4

$$\text{MSSQ} = \frac{2.64 \times (\text{total sickness score}) \times 9}{(\text{number of types of transportation experienced})} \tag{5.11}$$

$$\text{MSSQ raw score} = \text{MSSQ}_\text{A} + \text{MSSQ}_\text{B} \tag{5.12}$$

For the MSAQ, the 16 statements are divided into 4 subcomponents that examine various types of motion sickness. The scores for the subcomponents are calculated as the percentage of points earned

within each factor. The equation for the Gastrointestinal subcomponent is shown in Equation 5.13, the others are shown in Appendix D. The overall motion sickness score is obtained by calculating the percentage of total points scored, shown in Equation 5.14.

The results have a mean of 31.76 with a standard deviation of 16.07. The distribution of the results of the MSAQ is shown in Figure 5.21b.

$$\text{Gastrointestinal} = \frac{\text{sum of gastrointestinal items}}{36} \times 100 \tag{5.13}$$

$$\text{Overall score} = \frac{\text{sum of points from all items}}{144} \times 100 \tag{5.14}$$

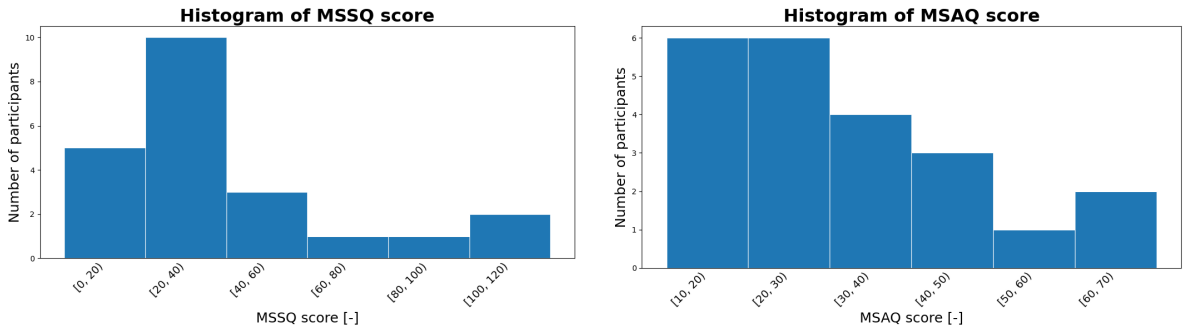

(a) Frequency distribution of the MSSQ scores

(b) Frequency distribution of the MSAQ scores

Figure 5.21: Histograms of questionnaire scores

The MSSQ and MSAQ scores for each participant are shown in Figure 5.22. Although the scale magnitudes differ between the two measures, the MSSQ and MSAQ show a positive relationship: people who are highly susceptible, as measured by the MSSQ, also tend to display greater motion sickness severity, as measured by the MSAQ. Subjects P01, P06, P13, P19, and P21 showed greater susceptibility, and P01, P11, P15, P19, and P21 also showed more severe symptoms at the end of the experiment. The correlation between the two questionnaires is displayed in Figure 5.23. The Spearman correlation coefficient equals 0.773, meaning a strong correlation.

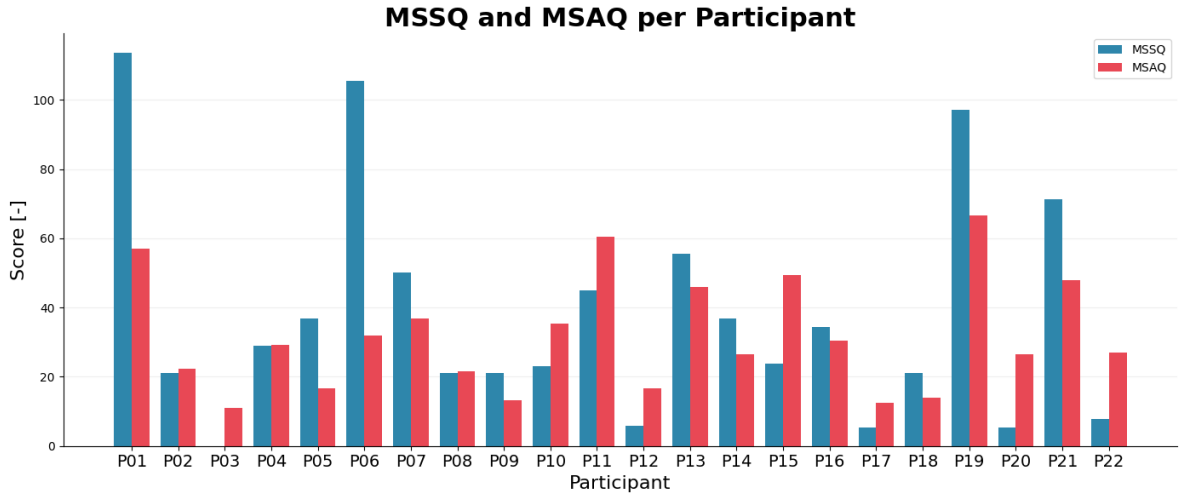

Figure 5.22: MSSQ and MSAQ scores per participant.

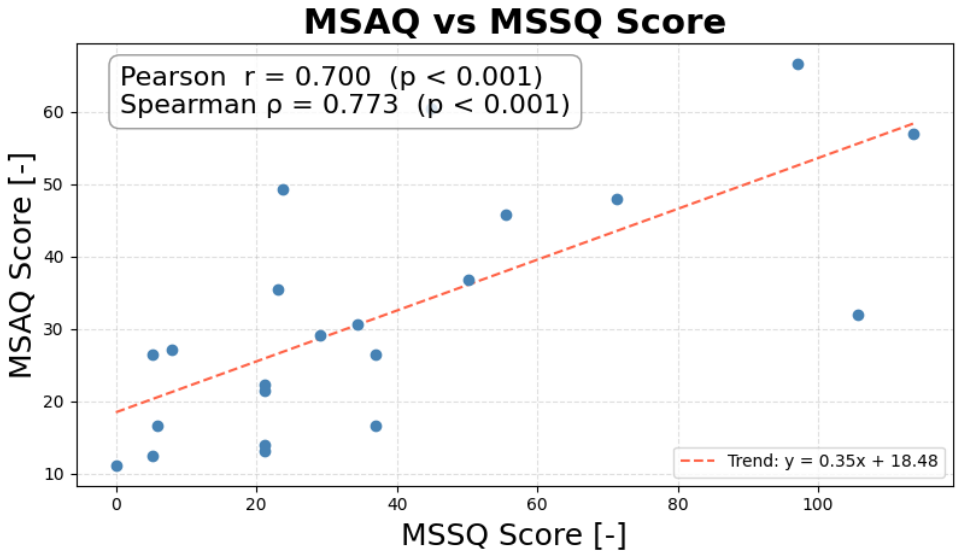

Figure 5.23: Correlation between MSAQ and MSSQ scores

5.6. MISC and Questionnaires

As a sanity check, the correlation between the MISC scores and the MSSQ and MSAQ scores is determined. The results are shown in Figure 5.24a and Figure 5.24b, respectively. The graphs showing the correlation between the final MISC score and the questionnaires are shown in Figure A.32 and Figure A.33. MISC and MSSQ have a Spearman correlation coefficient of 0.593, while MISC and MSAQ have a Spearman correlation coefficient of 0.828. Both indicate high correlation, as expected.

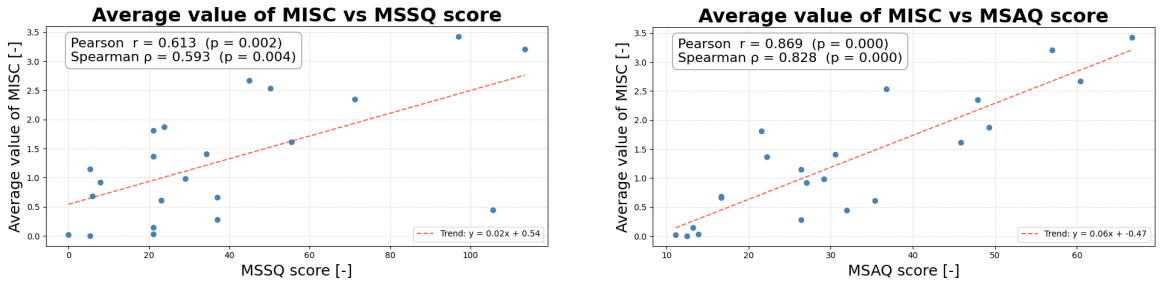

(a) Correlation between the average value of MISC and MSSQ scores

(b) Correlation between the average value MISC and MSAQ scores

Figure 5.24: Correlations between MISC and Questionnaire scores

5.7. MISC and sway

The correlation between the sway index and the average of the MISC scores and the final MISC score is shown in Figure 5.25a and Figure 5.25b, respectively. The z-score of the overall sway, as discussed in Subsection 5.1.3, is used again for the correlation analysis. The Spearman correlation between the average of MISC and the overall sway is 0.263, while the Spearman correlation between the final value of MISC and the overall sway is 0.095. Both indicate low correlation.

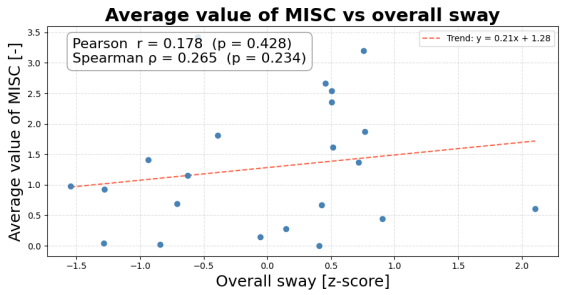

(a) Correlation between the average value of the MISC score and the overall sway index

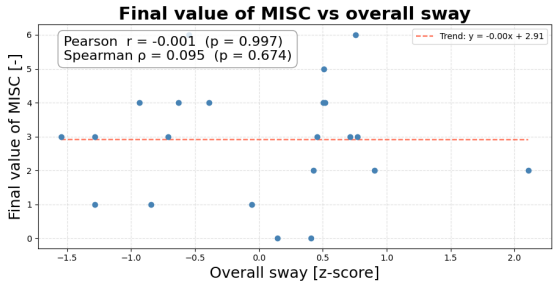

(b) Correlation between the final value of MISC score and the overall sway index

Figure 5.25: Correlation between MISC and overall sway

As discussed in Subsection 5.1.5, an increase in sway after motion sickness exposure was seen, specifically in the Stan EO condition. The correlation between the ratio after/before MS exposure of sway, indicating the difference of sway between before and after motion sickness exposure, and the average of the MISC scores and the final MISC score is shown in Figure 5.26a and Figure 5.26b, respectively. They have Spearman correlation coefficients of 0.034 and -0.013, respectively. Both indicate low correlation.

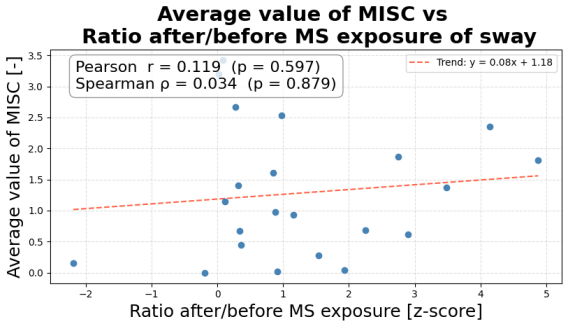

(a) Correlation between the average of MISC scores and the ratio after/before MS exposure of sway

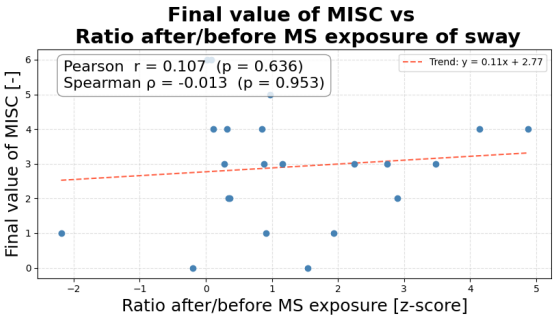

(b) Correlation between the final value of the MISC score and the ratio after/before MS exposure of sway

Figure 5.26: Correlation between MISC and the ratio after/before MS exposure of sway

As the SD_ML and MV_ML metrics in the Stan EO condition were the most significant, the correlation of these with the MISC score is analyzed. Figure 5.27a and Figure 5.27b show these results. The SD_ML metric has a Spearman correlation coefficient of 0.288, whereas MV_ML has 0.040. Both indicate low correlation, and neither reached significance.

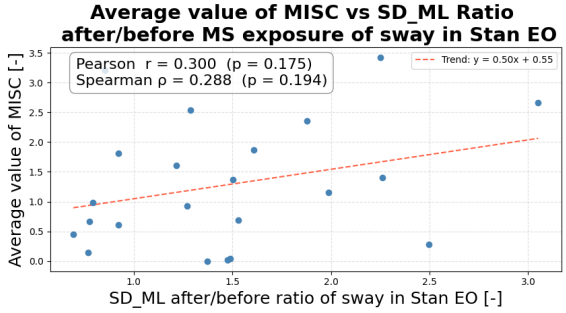

(a) Correlation between the average value of the MISC scores and SD_ML after/before ratio in Stan EO condition

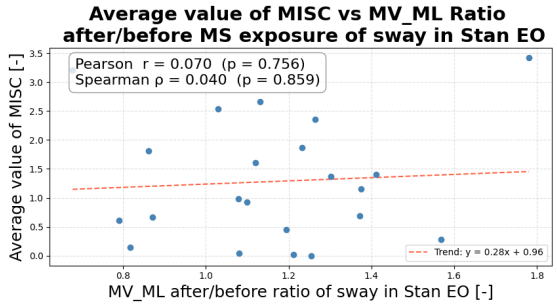

(b) Correlation between the average value of the MISC score and MV_ML after/before ratio in Stan EO condition

Figure 5.27: Correlation of the average of MISC score and SD_ML and MV_ML after/before ratio in Stan EO condition

As shown on Figure 5.4, P10 has an unusually high sway (> 2· SD) after motion sickness exposure. Therefore, the analysis of the difference between before and after MS exposure and the relation between sway increase and MISC is done both with and without P10. These results are presented in Table B.3 and Table B.4, respectively.

Spearman correlations were computed between the before-to-after ratio of each sway metric and the MISC score for each of the four conditions (*Stan EO, Stan EC, Sit EO, Sit EC*) separately. With all 22 participants included, no significant correlations were found. In the Standing with Eyes-Closed condition, the strongest correlations were observed for SD_AP (ρ = 0.40, p = 0.064) and MV_ML (ρ = 0.40, p = 0.064). These show moderate positive associations with the MISC score, but they are not significant. Excluding P10 from the analysis, two significant correlations were found in the Stan EC condition: SD_AP (ρ = 0.49, p = 0.024) and MV_ML (ρ = 0.44, p = 0.044). These results suggest that subjects who reported higher levels of motion sickness in the simulator tended to have a larger post-exposure increase in the anteroposterior sway amplitude and the mediolateral sway velocity, particularly in the Stan EC condition. None of the other conditions showed significant correlations in either analysis.

Furthermore, to assess whether sway can serve as an indicator of motion susceptibility, the correlation between the MISC score and the sway z-score *before* MS exposure was determined. Figure 5.28a and Figure 5.28b show this correlation for the average value and the final value of the MISC score, respectively. The Spearman correlation coefficient between the average of MISC and the sway before exposure is 0.050, and the Spearman correlation coefficient between the final MISC value and the sway is -0.127. Both indicate low correlation.

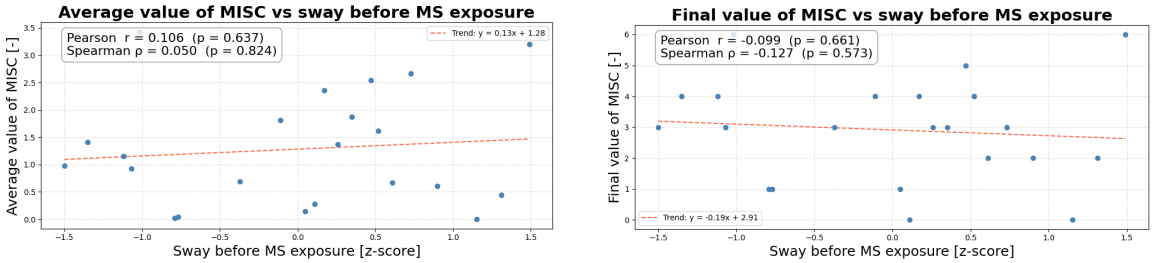

(a) Correlation between the average value of the MISC score and Sway before MS exposure (z-score)

(b) Correlation between the final value of MISC score and sway before MS exposure (z-score)

Figure 5.28: Correlation between MISC and sway before MS exposure

5.8. MISC and dynamic stabilization

The correlation between the TPL and Mean Displacement during dynamic stabilization and the average of the MISC scores is shown in Figure 5.29a and Figure 5.29b, respectively. The average of MISC vs TPL of dynamic stabilization has a Spearman correlation coefficient of 0.117, while the final value of MISC and the mean displacement of dynamic stabilization have a Spearman correlation coefficient of 0.119. Both indicate a low correlation.

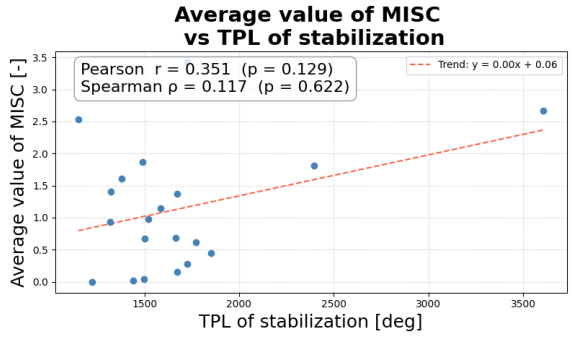

(a) Correlation between the average value of the MISC score and TPL during dynamic stabilization

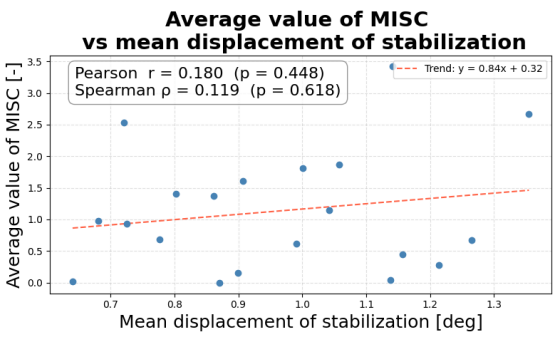

(b) Correlation between the average value of the MISC score and the mean Displacement during dynamic stabilization

Figure 5.29: Correlation between the average of MISC and TPL and Mean Displacement during dynamic stabilization

Additionally, the correlation between the velocity in both the AP and ML direction and the MISC scores is shown in Figure 5.30a and Figure 5.30b, respectively. No strong correlation is found as MV_AP has a Spearman correlation of 0.253 with the MISC score, and MV_ML has a coefficient of 0.253.

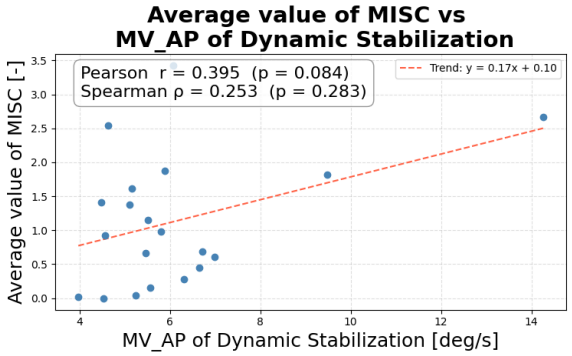

(a) Correlation between the average value of the MISC score and MV_AP during dynamic stabilization

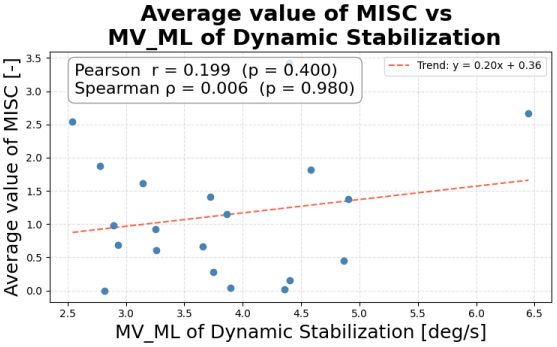

(b) Correlation between the average value of the MISC score and MV_ML during dynamic stabilization

Figure 5.30: Correlation between the average of MISC and MV_AP and MV_ML during dynamic stabilization

The composite dynamic stabilization index was calculated in Section 5.2, and the results are shown in Figure 5.12. The correlation between this composite dynamic stabilization index and the average and final MISC score is shown in Figure 5.31a and Figure 5.31b, respectively. Both show low, non-significant correlations: the average MISC score has a Spearman correlation of 0.135, and the final MISC score has a Spearman correlation of -0.058.

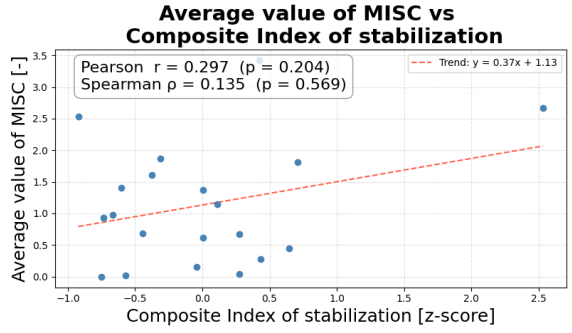

(a) Correlation between the average value of the MISC score and the z-score of dynamic stabilization

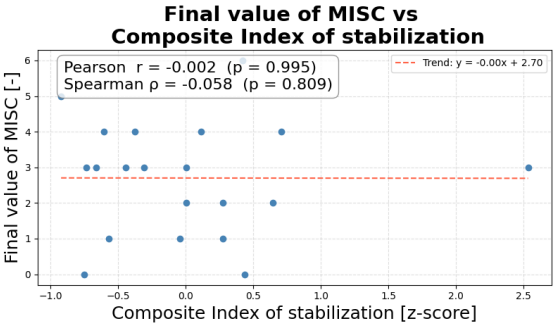

(b) Correlation between the final value of the MISC score and the z-score of dynamic stabilization

Figure 5.31: Correlation between the average of MISC and Composite dynamic stabilization index

The Spearman correlation coefficients between each dynamic stabilization metric and the MISC score are shown in Table B.9, and in Table B.8 excluding P11, to analyze the effect of the outlier. In both cases, none of the correlation coefficients is statistically significant. Furthermore, removing P11 does not noticeably affect these results. However, removing P11 from the data reduces the variance of the MV_AP and TPL metrics, without revealing any new significant results. These results suggest that the head stabilization during dynamic movement is not significantly related to the level of motion sickness experienced.

5.9. MISC and motion perception

The correlation between the velocity storage time constant and the average of the MISC scores and the final MISC score is shown in Figure 5.32a and Figure 5.32b, respectively. The average value of MISC and the velocity storage time constant have a moderate positive Spearman correlation coefficient (ρ = 0.528, p = 0.012), and the final value of MISC and the velocity storage time constant also showed a moderate positive Spearman correlation coefficient (ρ = 0.433, p = 0.044). Both correlations were statistically significant (p < 0.05), suggesting that a longer velocity storage time constant is associated with greater motion sickness severity.

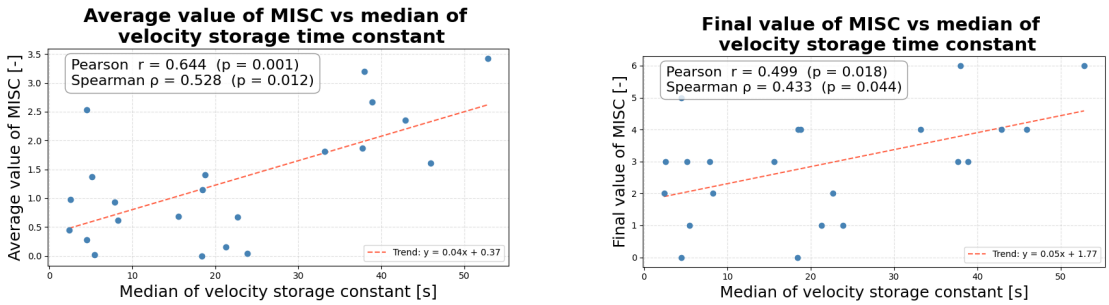

(a) Correlation of the average value of the MISC score and the median of velocity storage time constant

(b) Correlation of the final value of the MISC score and the median of the velocity storage time constant

Figure 5.32: Correlation between MISC and velocity storage time constant

5.10. Correlation between all the metrics

The matrix shown in Figure 5.33 displays Spearman correlation coefficients between all variables. Darker colors indicate stronger correlations; dark red indicates a very strong positive correlation, and dark blue indicates a very strong negative correlation. The asterisks denote statistical significance after Bonferroni correction for the 151 pairs (* p_$bonf$ < 0.05, ** p_$bonf$ < 0.01). The amplitude metrics for sway (SD and MV in both planes) show strong positive correlations and correlate positively with both TPL and the Z-index, with several exceeding the Bonferroni threshold. The dynamic Stabilization metrics also show strong correlation with each other. The MSSQ and MSAQ are strongly correlated with each other (ρ = 0.77, p_$bonf$ < 0.001). The MSAQ also shows strong correlation with the average MISC (ρ = 0.83, p_$bonf$ < 0.001). No strong correlations are found between the MISC and the postural sway or dynamic stabilization metrics.

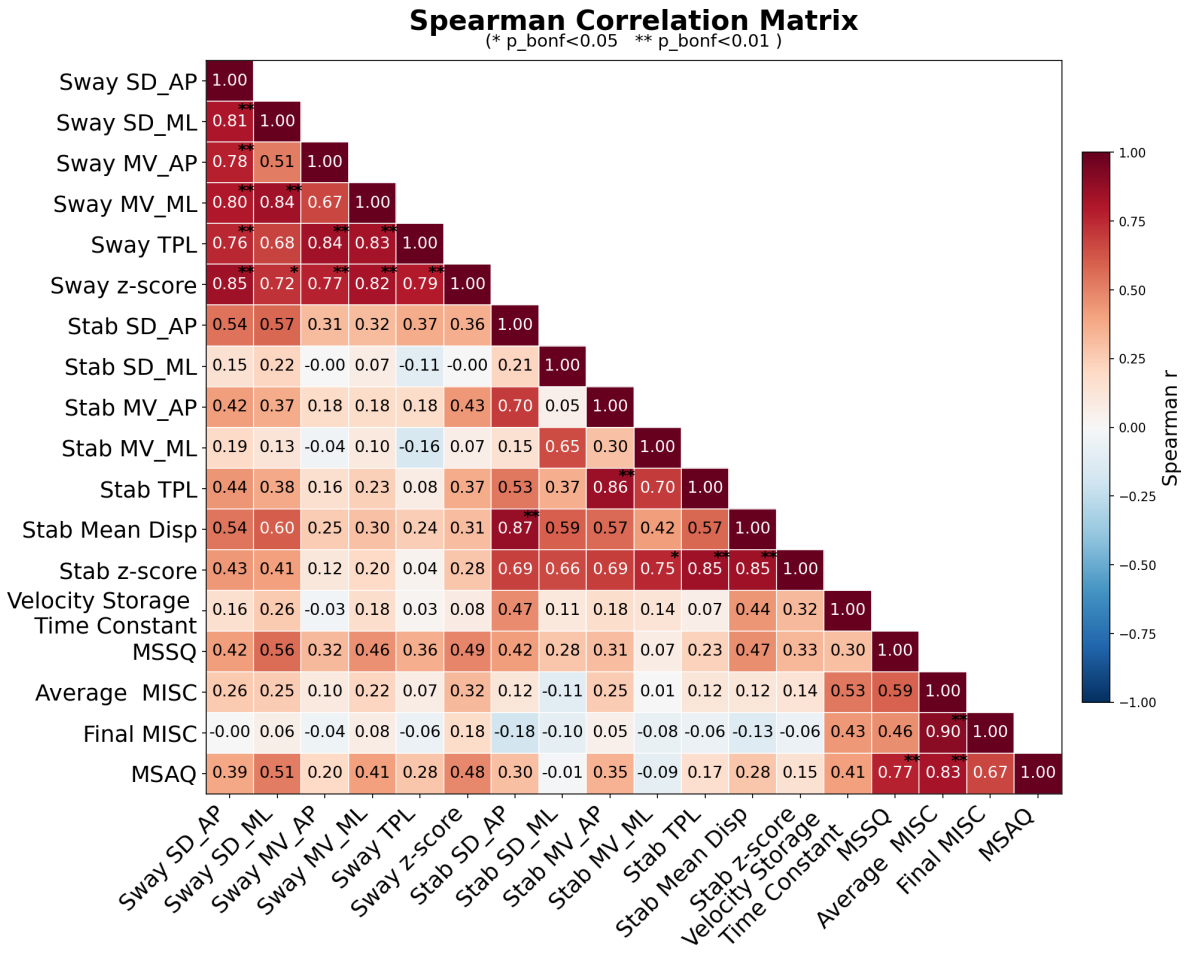

Figure 5.33: Spearman correlation matrix between all the metrics: Sway, Dynamic Stabilization, Motion Perception, Motion Sickness, Questionnaires.
Bonferroni correction (α = 0.05/171 $\approx$ 0.00029), * p_{bonf} <0.05, ** p_{bonf} <0.01

6

Discussion

This thesis investigated whether individual differences in motion perception and postural stability relate to motion sickness susceptibility, specifically during exposure to controlled-vehicle motion. A within-subjects experiment was conducted in which 22 healthy participants completed postural sway tests, a rotational motion perception task, a dynamic head stabilization task, and a motion sickness exposure test. Below, the experimental approach is discussed, followed by an interpretation of the main findings in relation to the existing literature, possible explanations for similarities and differences, and the research questions and answers. Finally, limitations and implications of the experimental results are considered and suggestions for future research are provided.

Experimental protocol

Overall, the experimental protocol was carried out largely as planned, and participants completed all test conditions. However, some practical considerations should be taken into account when interpreting the results.

During sway measurements, particularly during standing, some participants exhibited brief but large voluntary movements. Even though filtering was used to remove voluntary movements, this may still influence the final sway values for these individuals. This is inevitable as participants were clearly instructed to stabilize their posture, but instruction is inherently difficult to enforce without biofeedback. Further studies could address this by including stricter exclusion criteria based on specific movements.

During the motion perception experiment and the dynamic stabilization test, a recurring issue occurred with the XSENS sensors. As two were used to measure head and seat movement simultaneously, they were often difficult to connect reliably. Additionally, their attachment to the seat and head was not always secure, occasionally causing the sensors to fall off or lose vertical alignment. This was mainly mitigated by checking the sensors between trials and reattaching them. Still, since the sensors had to record long, large movements, residual noise from minor misalignment could not be fully excluded. In addition, the lever-based response during the motion perception experiment saturated at $\pm$ 45 degrees, and could therefore only report direction and relative intensity.

Furthermore, two participants had to be excluded from the dynamic stabilization analysis due to recording errors.

Postural sway

A first finding of sway was the correlation between height and sway. As shown in Table B.1, a slightly higher correlation was found in the standing conditions than in the sitting conditions. However, no meaningful correlation (ρ = -0.17, p = 0.455) was found in either condition. It can be concluded that height does not significantly affect an individual's sway.

Next, to further analyze postural sway, the internal structure of the findings of Luo et al. (2018) was replicated using the same metric set, consisting of five magnitude metrics (SD_AP, SD_ML, MV_AP,

MV_ML, TPL) and two complexity metrics (fApEn_AP, fApEn_ML). In addition, the composite index z-score was calculated to identify meaningful inter-individual differences in postural behavior.

The magnitude metrics were higher in standing than in sitting, indicating the greater demand on balance control while standing upright. In addition, eyes-closed standing was greater than eyes-open standing, supporting the literature on sensory reliance. This effect was not seen in the sitting conditions. This can be explained by the fact that postural instability is generated by standing, and sitting poses a less mechanical challenge than standing; thus, less benefit is gained from vision when sitting. Slightly higher fApEn values were observed in the sitting condition, suggesting more complex and adaptive postural control. This is in line with the findings of Luo et al. (2018), who interpret lower postural demands as leading to a more flexible neuromuscular system for control strategies [Luo et al., 2018].

After MS exposure, sway increased significantly for the *Stan EO* condition, specifically in the medio-lateral direction (SD_ML +37.6%, MV_ML +12.2%), while the neuromuscular complexity was reduced (fApEn_AP -3.5%, fApEn_ML -7.6%). No significant effects were observed in the seated conditions.

Another interesting finding is the lack of effect in the seated condition. This reflects how the seat back's support limits trunk motion and reduces active postural challenges, regardless of vestibular disturbance. A similar observation was reported by Mirakhorlo et al. (2022), who found that seat configuration modulated the transmission of whole-body vibration to the head and trunk [Mirakhorlo et al., 2022]. In this study, the seated condition was performed in a standard car seat without the headrest, which may have been sufficient passive support to reduce the effect of motion sickness on postural control.

Dynamic head stabilization

In response to whole-body perturbation induced by the Mirakhorlo motion during the dynamic head stabilization test, participants typically exhibited moderate head stabilization, although individual variation was observed. A mean displacement of 0.96 ± 0.21 deg indicates that the majority of participants maintained a neutral head position to a greater extent throughout this task.

A difference in mean velocity is observed between AP (6.12 deg) and ML (3.82 deg). This is consistent with the fact that the human spine allows more movement in forward and backward bending than in sideways bending.

As mentioned in Section 5.2, P11 stands out in all aspects, yielding a z-score of +2.53 based on the composite metric for the head motion. They show large amplitudes and low fApEn values in the AP direction, suggesting a reactive head-motion stabilization strategy, meaning head motion is corrected after the fact rather than before. P03 and P07 demonstrated head motion that approximates ideal behavior. They showed smaller head motion and higher fApEn values, indicating a feed-forward control of head motion.

Several limitations should be considered when interpreting these results. The IMU XSENS sensors were used, which can measure rotation accurately, although they are also prone to noise from minor motion and sensor drifting. This could have introduced noise during the measurements. Furthermore, only head rotation was analyzed, not translational motion. Therefore, the actual head movements are likely to be underestimated. Additionally, because of measurement errors, two participants had to be excluded from the sample. The sample was thus reduced, potentially affecting the generalizability of the group distribution.

Rotational motion perception

Individual rotational motion perception was analyzed by taking the median of the velocity storage time constant across the four trials for each participant. The average across participants was 21.34 seconds. This is slightly higher than the results reported by Irmak et al. (2021), who found a mean of 17.2 s (SD = 6.8 s), and Bertolini et al. (2011), who found a mean of 15.5 s (SD = 5 s). However, the average found in the current study still falls within the 10-30 second range reported by Bertolini et al. (2011) for healthy adults. It is important to note that both Irmak et al. and Bertolini et al. used different methods to determine the time constant, as discussed in Section 5.3, which may explain the difference in means [Irmak et al., 2021] [Bertolini et al., 2011]. Still, the results seem to be in an acceptable range. Furthermore, the subjects showed large variability, with the shortest reported perception being

1.2 seconds and the longest being over 5 minutes. These individual variabilities are also shown in the individual lever-angle plots in Section A.1.

Motion sickness

The motion exposure test did cause a progressive increase in sickness symptoms over the time period, with a mean final MISC of 2.9. Figure 5.17 shows a sawtooth pattern across laps, indicating that the ten-second inter-lap break provided only partial recovery. Two participants reached the maximum allowed MISC score of 6 at the end of the fifth lap, while three participants reported almost no symptoms at all. This shows the inter-individual variability in motion sickness.

The driving settings used in this experiment were taken from Kotian et al. (2025), which were an MPC-based MCA that prioritized specific force reproduction with a sensory conflict weight of zero. For these specific driving settings, Kotian et al. found a mean MISC of 3, which is similar to the 2.9 found in the current experiment [Kotian et al., 2025]. This confirms that the exposure was carried out as intended and that the results could be used for other studies.

Additionally, the MSAQ showed a strong correlation with the MISC score (ρ = 0.828), providing further evidence that self-reported susceptibility was associated with symptoms.

MSSQ

The MSSQ showed a positive correlation with the MISC score (ρ = 0.593). This aligns with previous findings that MSSQ has limited predictive validity for sickness under specific driving conditions. For example, Irmak et al. (2025) reported a correlation of 0.212 between the MSSQ and MISC during passive driving and suggest that it pools self-reported susceptibility across multiple modes of transport and stimulation types, rather than measuring susceptibility to a specific motion context [Irmak et al., 2025]. The higher correlations observed in this experiment may reflect the more controlled, provocatively designed driving conditions. The higher correlation between MSAQ and MISC is expected, as the MSAQ is filled out immediately after exposure. This reflects the specific symptom profile for that exposure rather than a lifetime average.

Furthermore, the MSSQ and MSAQ questionnaires showed a strong correlation (ρ = 0.773), supporting the validity of their measures of susceptibility and symptoms.

Relationship between motion perception and motion sickness

The most important finding from the motion perception analysis is that the velocity storage time constant showed a statistically significant positive correlation with the severity of motion sickness (Spearman ρ = 0.528, p = 0.012 for the average MISC; Spearman ρ = 0.433, p = 0.044 for the final MISC). This finding suggests that individuals who continue to perceive rotation longer after deceleration tend to experience greater motion sickness, specifically during simulator driving.

Notably, both motion perception and motion sickness show a similar inter-individual variability. Motion perception has a CV of 0.72, whereas the average MISC score has a CV of 0.80. These comparable coefficients suggest that the variability in motion perception resembles the variability in motion sickness,

This is consistent with the findings of Dai et al. (2003), who reported a negative correlation between the number of tolerated head movements and the velocity storage time constant. Furthermore, their study found a decrease in velocity storage time constants across sessions, as participants habituated to the stimuli. This suggests that longer time constants indicate greater vulnerability to motion sickness from rotational stimuli [Dai et al., 2003].

However, Irmak et al. (2021) found a weaker and non-significant correlation between the velocity storage time constant and motion sickness sensitivity. They explained this finding by stating that they only used pure fore-aft translation stimulus. Additionally, their sample was relatively small. Therefore, the velocity storage constant may be a good indicator of susceptibility to motion sickness, given that the stimulus has a rotational component and a larger sample size is used.

Relationship between sway and motion sickness

To examine the idea using sway as an indicator for motion sickness susceptibility, the correlation between sway before MS exposure and the MISC level was determined. No correlation was found (ρ = 0.050 for average MISC; ρ = -0.127 for final MISC), indicating that changes in time of sway is not a good indicator for motion sickness susceptibility.

The fact that no significant effect of motion sickness on sway is found is surprising, especially since Riccio and Stoffregen (1991) argued that postural stability is not only a consequence of motion sickness but a 'necessary precursor of motion sickness' [Riccio and Stoffregen, 1991]. Furthermore, Stoffregen and Smart (1998) confirmed in their experiment that postural instability precedes motion sickness [Stoffregen and Smart, 1998]. In this experiment, no support for this was found. A possible explanation for this absence is that the experiment used static conditions to measure sway, whereas Stoffregen and Smart (1998) used a moving-room paradigm.

In Table B.3, presenting the before-to-after ratios for all conditions, it can be seen that only the Stan EO condition showed significant changes between before and after motion sickness exposure. Specifically, the SD_ML (mean = 1.4733, p = 0.0021) has an increase of 47.3%, and the MV_ML (mean = 1.16, p = 0.0094) has an increase of 16% sway. In either sitting condition, while almost all metrics increased except MV_ML, no significant changes were observed, as the changes were small or negligible. Furthermore, no change was significantly correlated with MISC scores for any of the conditions. Showing that there is no correlation between how much a participant's sway has changed and the level of sickness they reported.

P10 showed unusually high sway after MS exposure, most likely due to a measurement error. Because of that, a sensitivity analysis was performed excluding P10, and the results are presented in Table B.4. The significant increase, shown in Table B.3, in SD_ML (mean = 1.473, p = 0.0021) and MV_ML (mean = 1.160, p = 0.0094) remained when excluding P10 (SD_ML: mean = 1.499, p = 0.0018; MV_ML: mean = 1.178, p = 0.0047), confirming these effects are not driven by P10. However, excluding P10 showed moderate correlations between MISC and the sway ratio in the Stan EC condition SD_AP (ρ = 0.4896, p = 0.024) and MV_ML (ρ = 0.4429, p = 0.044). This result shows that people who reported more severe MS symptoms showed a larger increase in anteroposterior sway amplitude and mediolateral velocity while standing with eyes closed. To account for multiple comparisons, a Bonferroni correction was applied across all 28 sway measures included in the correlation analysis (α = 0.05/28 = 0.00179). None of the 28 correlations reached this corrected threshold, including those that appeared significant before correction. Therefore, the primary conclusion that sway does not meaningfully correlate with motion sickness severity remains.

However, even though no effect of motion sickness was found, a change in sway before and after is observed across almost every metric in all conditions. More specifically, based on the combined sway response across all five magnitude metrics, the composite ratio confirms that this increase was specific to standing rather than a general effect: the standing-only composite showed a significant increase (mean = 1.150, p = 0.0143), while the sitting-only composite showed no change (mean = 1.066, p = 0.388). A possible explanation is that, before the first set of sway tests, participants were in motion while traveling to the setup, whereas before the second set of measurements, they were seated for more than 30 minutes. This might indicate that muscle activation is necessary to maintain better postural stability, independent of MS exposure.

Answers to hypothesis

The hypothesis stated that individuals with greater postural sway, reduced head stabilization, and a larger velocity storage time constant exhibit higher levels of motion sickness symptoms. In this study, individuals with a larger velocity storage time constant experienced more severe motion sickness symptoms. A moderate but significant correlation was found between them. No influence of postural sway on motion sickness was found. Sway increased after motion sickness exposure across the group, but did not predict which individuals would become sick. Additionally, no significant correlation was found between the dynamic head stabilization and motion sickness severity. Dynamic and static stabilization show a moderate correlation, as shown in Figure 5.33, suggesting shared underlying postural mechanisms. The use of Mirakhorlo's motion allows dynamic stabilization to be further analyzed across the

x, y, and z axes and rotation in the frequency domain; however, this is beyond the scope of this thesis. Irmak et al. (2020) similarly studied head roll as an indicator of postural stability during a sickening drive and reported effects of sway on motion sickness that did not reach significance, which was likely due to the small sample size and noisy data during high lateral accelerations [Irmak et al., 2020]. Thus, the current hypotheses can be partially supported, as the velocity storage constant may predict motion sickness susceptibility, whereas no significant correlations were found for postural sway or head stabilization.

Limitations

The study has several limitations. First, the sample size of 22 subjects is modest. This leads to several analyses being sensitive to the inclusion or exclusion of outliers, as shown when P10 is excluded in sway analysis. Therefore, significant results should be considered uncertain, and non-significant results cannot be considered as definitive proof for no effect, since the study was most likely underpowered to detect small correlations reliably.

Next, the sample consisted of young adults aged 18-34 years, limiting generalizability to broader age groups. Motion sickness is known to vary, among others, with age and sex, as postural control and vestibular sensitivity change over the lifetime and are affected by training. A more representative sample is needed to draw general conclusions about predictive values by age or sex.

Furthermore, the measurements may contain noise as the XSENS sensors are not flawless and sensitive to small movements. The headband used to attach the sensor to the subjects was not small enough to prevent the sensor from making small extra movements, which may affect the final data.

Finally, given the within-subjects design of the experiment, in which participants were exposed to the tasks in a fixed order, it is not entirely possible to exclude carryover effects. For instance, since the motion perception assessment was performed before the motion sickness exposure, this may have affected the severity of the reported symptoms.

Implications and Future research

The most important finding of this study is the significant correlation between the motion sickness level and the velocity storage time constant. The EVAR paradigm is simple, non-nauseating when performed correctly, and can be completed in under 15 minutes. This allows it to be used as a pre-ride screening tool.

Practically, this finding is particularly valuable when testing motion sickness mitigation strategies, as individuals with very low susceptibility are not informative, since they are unlikely to experience sickness regardless of the intervention. This makes it difficult to detect any beneficial effect. Conversely, individuals with extremely high susceptibility are also not ideal since they tend to become sick too quickly and too severely to allow for meaningful or complete evaluation of the mitigation strategy. Therefore, the EVAR paradigm could screen subjects in advance, enabling researchers to recruit a more targeted sample of moderately susceptible individuals who are more likely to properly evaluate the interventions and mitigation strategies.

However, the MSSQ remains the most accurate predictor of motion sickness susceptibility, as evidenced by the higher correlation observed in this study. The EVAR paradigm should therefore not be seen as a replacement, but rather as a complementary method. Combining the two methods may offer a more robust pre-screening approach.

The postural sway under static conditions did not predict susceptibility. This suggests that this is an insufficient tool to use as a standalone screening measure. However, sway increased after motion sickness, but no significant correlation was found between sway and motion sickness. This could indicate that a type of muscle activation before a test improves postural stability, whereas sitting still for a period may reduce it.

The postural dynamic stabilization could be analyzed across the frequency domain in the x-, y-, and z-axes and in rotation. This could lead to finding postural strategies, specific to each frequency, and may help predict motion sickness susceptibility. However, this analysis ,is outside the scope of this

study. Further, the data collected and presented in this thesis related to motion perception, postural stability and motion sickness could be used as a dataset for future use.

The most important note for future research is replication with a larger, more diverse sample, both age- and sex-wise, which would reduce sensitivity to outliers and provide more insights into individual differences. With a larger sample, randomizing the task order across participants might also help exclude carryover effects from the motion perception test on subsequent sickness responses.

Finally, replacing the single head-mounted IMU sensors with a full-body XSENS suit would allow whole-body kinematics analysis. This can provide a broader and clearer idea of individual postural strategies.

Conclusion

In conclusion, this thesis investigated individual differences in postural stability in both static and dynamic conditions and in rotational motion perception, and investigated their relation to motion sickness susceptibility during controlled vehicle motion. A within-subject experiment was conducted in which 22 healthy adults performed a series of experiments in the same order: postural sway measurements, a rotational motion perception task, a dynamic stabilization task, and a motion sickness exposure test.

The primary result of this study is a statistically significant correlation between the velocity storage time constant and motion sickness severity in individuals (Spearman ρ = 0.528, p = 0.012), suggesting that individuals who perceived longer rotation after deceleration also reported more severe motion sickness symptoms during simulator driving. This suggests the Earth Vertical Axis Rotation paradigm, which is short, non-nauseating, and feasible, as an interesting tool for screening individuals for motion sickness susceptibility. In practice, such a tool would be useful for identifying a moderate-susceptibility sample for use in motion sickness mitigation studies. The MSSQ, however, appears to still be a better predictor of susceptibility, so a combination of both might be the best solution.

Postural sway did not show a strong correlation with motion sickness severity. However, sway increased after motion sickness exposure, both in amplitude and velocity, across all standing conditions, with a significant increase in the eyes-open condition. This suggests that exposure to motion sickness or, potentially, just a 30 min sitting period affected individuals' sway. However, the sway measured before the MS exposure did not correlate with MS severity, suggesting that sway is not a good individual predictor of motion sickness susceptibility. Additionally, no significant correlation was found between head stability during whole-body dynamic perturbation and motion sickness susceptibility.

The MSSQ and MSAQ showed strong positive correlations with each other and with the reported MISC score. This supports their validity as an additional screening method.

In summary, the hypothesis that greater postural sway, reduced dynamic head stabilization, and a larger velocity storage time constant can help predict susceptibility to motion sickness is only partially supported, as only a statistically significant correlation was found between the velocity storage time constant and MISC score. However, the correlation was not significant under the Bonferroni correction ($\alpha = 0.00029$), suggesting that this finding should be interpreted with caution, and replicated with a larger sample size before drawing final conclusions. Furthermore, postural sway and dynamic stabilization did not show a meaningful correlation with motion sickness susceptibility for the specific conditions in this experiment.

These findings contribute to the growing understanding of individual factors related to motion sickness susceptibility and may provide new ways for future motion sickness mitigation strategies in automated vehicles and virtual reality environments.

7

Acknowledgments

I would like to express my gratitude to my supervisors, Professor Happee and Dr. Kotian, for their assistance and support throughout my thesis. Their feedback and guidance helped me improve the quality of this research and its approach to the problem.

I am also thankful to everyone who helped me during the practical execution of this project, specifically Maurits Pfaff and Roel Trachsler, and Kseniia Khomenkom, for providing technical support whenever I needed it and for helping me figure out how to work with the rotational chair and the sensors. I would also like to thank Hsiang-Yu Chen for helping me code the rotational chair to achieve the desired results. And, of course, thank you to all the participants who made this experiment possible.

Lastly, I would also like to thank my fellow students and friends for the interesting conversations, coffee breaks, and support they offered me along the way. These moments made the thesis process more enjoyable and helped me stay motivated. Lastly, I would like to express my deepest gratitude to my family for all their support, patience, and encouragement during my studies. Their support has been vital to me not only throughout this thesis but also during my entire stay at TU Delft.

References

Bertolini, G. et al. (2011). “Velocity storage contribution to vestibular selfmotion perception in healthy human subjects”. In: *Journal of neurophysiology* 105, pp. 209–223. ISSN: 1664-2295. DOI: 10.1152/jn.00154.2010.

Bos, J.E. and Bles, W. (1998). “Modelling motion sickness and subjective vertical mismatch detailed for vertical motions”. In: *Brain Research Bulletin* 47.5, pp. 537–542. ISSN: 0361-9230. URL: https://www.sciencedirect.com/science/article/pii/S0361923098000884.

Chang, E, Kim, H. T., and Yoo, B (2020). “Virtual Reality Sickness: A Review of Causes and Measurements”. In: *International Journal of Human–Computer Interaction* 36.17, pp. 1658–1682. DOI: 10.1080/10447318.2020.1778351.

Dai, M. et al. (July 2003). “The relation of motion sickness to the spatial?temporal properties of velocity storage”. In: *Experimental Brain Research* 151.2, pp. 173–189. DOI: 10.1007/s00221-003-1479-4. URL: https://doi.org/10.1007/s00221-003-1479-4.

de Winkel, K. N. et al. (2022). “Relating individual motion sickness levels to subjective discomfort ratings.” In: *Experimental Brain Research* 240.4, pp. 1231–1240. DOI: 10.1007/s00221-022-06334-6.

Golding, J. F. (1998). “Motion sickness susceptibility questionnaire revised and its relationship to other forms of sickness”. In: *Brain Research Bulletin* 47.5, pp. 507–516. ISSN: 0361-9230. DOI: 10.1016/S0361-9230(98)00091-4. URL: https://www.sciencedirect.com/science/article/pii/S0361923098000914.

— (2006a). “Motion sickness susceptibility”. In: *Autonomic Neuroscience* 129.1. Nausea and Vomiting: An Interdisciplinary Approach, pp. 67–76. ISSN: 1566-0702. URL: https://www.sciencedirect.com/science/article/pii/S1566070206002128.

— (2006b). “Predicting individual differences in motion sickness susceptibility by questionnaire”. In: *Personality and Individual Differences* 41.2, pp. 237–248. DOI: 10.1016/j.paid.2006.01.012.

Irmak, T., de Winkel, K. N., and Happee, R. (2025). “Visually induced motion sickness correlates with on-road car sickness while performing a visual task”. In: *Experimental Brain Research* 243.81. DOI: 10.1007/s00221-025-07020-z.

Irmak, T., Pool, D. M., and Happee, R. (Nov. 2020). “Objective and subjective responses to motion sickness: the group and the individual”. In: *Experimental Brain Research* 239.2, pp. 515–531. DOI: 10.1007/s00221-020-05986-6. URL: https://doi.org/10.1007/s00221-020-05986-6.

Irmak, T. et al. (2021). “Individual motion perception parameters and motion sickness frequency sensitivity in fore-aft motion.” In: *Exp Brain Res* 239, pp. 1727–1745. DOI: 10.1007/s00221-021-06093-w.

Keshner, E. A. (2000). “Modulating active stiffness affects head stabilizing strategies in young and elderly adults during trunk rotations in the vertical plane”. In: *Gait & Posture* 11.1, pp. 1–11. ISSN: 0966-6362. URL: https://www.sciencedirect.com/science/article/pii/S0966636299000466.

Keshner, E. A., Cromwell, R., and Peterson, B. (June 1995). “Mechanisms controlling human head stabilization. II. Head-neck characteristics during random rotations in the vertical plane”. In: *Journal of neurophysiology* 73, pp. 2302–2312. DOI: 10.1152/jn.1995.73.6.2302.

Keshner, E. A. and Peterson, B. (July 1995). “Mechanisms controlling human head stabilization. I. Head-neck dynamics during random rotations in the horizontal plane”. In: *Journal of neurophysiology* 73, pp. 2293–301. DOI: 10.1152/jn.1995.73.6.2293.

Kotian, V. et al. (2025a). *“Impact of Physical and Visual Motion on Subjective Perception of Vertical Orientation”*.

Kotian, V. et al. (2025b). “Reducing Discomfort in Driving Simulators: Motion Cueing for Motion Sickness Mitigation”. PhD dissertation. Delft, the Netherlands: Technical University of Delft.

LawInfo Staff (2024). *How Many Car Accidents Are Caused by Human Error?* URL: https://www.lawinfo.com/resources/car-accident/how-many-car-accidents-are-caused-by-human-er.html.

Luo, H. et al. (2018). “The Effect of Visual Stimuli on Stability and Complexity of Postural Control”. In: *Frontiers in Neurology* Volume 9 - 2018. ISSN: 1664-2295. DOI: 10.3389/fneur.2018.00048.

Martínez-Díaz, M. and Soriguera, F. (2018). “Autonomous vehicles: theoretical and practical challenges”. In: *Transportation Research Procedia* 33. XIII Conference on Transport Engineering, CIT2018, pp. 275–282. ISSN: 2352-1465. DOI: https://doi.org/10.1016/j.trpro.2018.10.103. URL: https://www.sciencedirect.com/science/article/pii/S2352146518302606.

Mirakhorlo, M. et al. (2022). “Effects of seat back height and posture on 3D vibration transmission to pelvis, trunk and head”. In: *International Journal of Industrial Ergonomics* 91. DOI: 10.1016/j.ergon.2022.103327.

Olnick, A. and Lubow, R. E. (Sept. 1991). “Why is the driver rarely motion sick? The role of controllability in motion sickness.” In: *Ergonomics*, pp. 867–879. DOI: 10.1080/00140139108964831.

Riccio, G. E. and Stoffregen, T. A. (1991). “An ecological theory of motion sickness and postural instability”. In: *Ecological Psychology* 3, pp. 195–240. DOI: 10.1207/s15326969eco0303_2.

Sherman, Craig R. (Mar. 2006). “Motion Sickness: Review of causes and Preventive strategies”. In: *Journal of Travel Medicine* 9.5, pp. 251–256. DOI: 10.2310/7060.2002.24145. URL: https://doi.org/10.2310/7060.2002.24145.

Stoffregen, T. A. and Smart, L. J. (1998). “Postural instability precedes motion sickness”. In: *Brain Research Bulletin* 47.5, pp. 437–448. ISSN: 0361-9230. URL: https://www.sciencedirect.com/science/article/pii/S0361923098001026.

Stoffregen, T. A. et al. (2000). “Postural instability and motion sickness in a fixed-based flight simulator”. In: *Human factors* 42, pp. 458–469. DOI: 10.1518/001872000779698097.

WHO (2023). *Road traffic injuries*. URL: https://www.who.int/news-room/fact-sheets/detail/road-traffic-injuries.

Xsens Technologies B.V. (2020). *Xsens DOT User Manual*. Accessed: 2026-05-26. URL: https://www.xsens.com/hubfs/Downloads/Manuals/Xsens%20DOT%20User%20Manual.pdf.

A

Figures

Figure A.1: Participant set-up for the rotational motion perception test, including a blindfold, noise-canceling headphones, a handheld response lever, and an IMU sensor placed on the head

A.1. Motion Perception - Lever angle

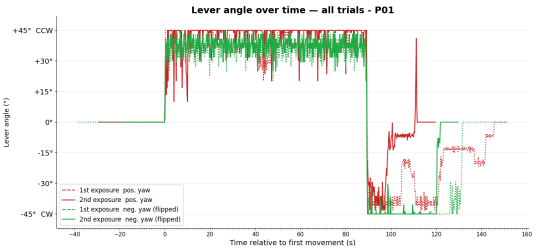

Figure A.2: Motion Perception - Lever Angle of P01

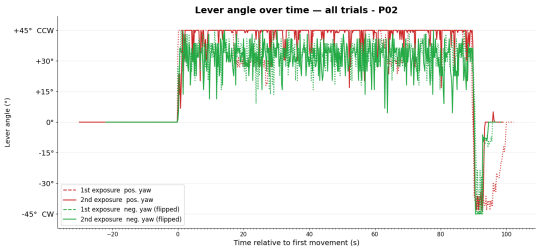

Figure A.3: Motion Perception - Lever Angle of P02

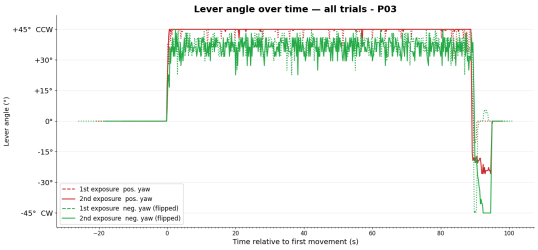

Figure A.4: Motion Perception - Lever Angle of P03

Figure A.5: Motion Perception - Lever Angle of P04

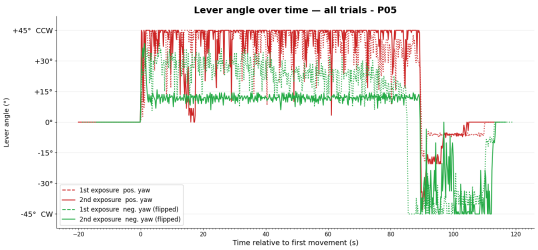

Figure A.6: Motion Perception - Lever Angle of P05

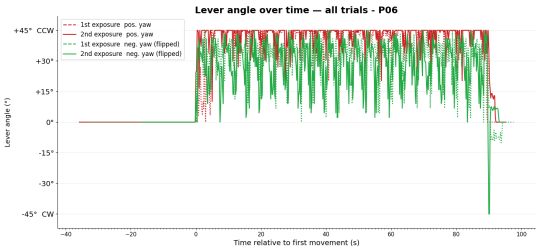

Figure A.7: Motion Perception - Lever Angle of P06

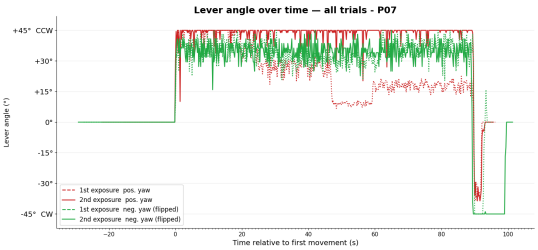

Figure A.8: Motion Perception - Lever Angle of P07

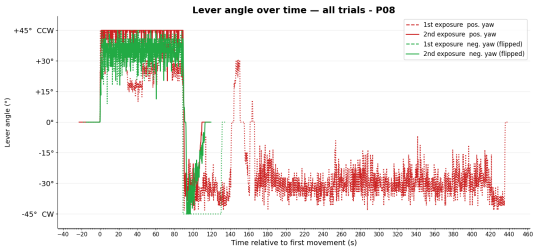

Figure A.9: Motion Perception - Lever Angle of P08

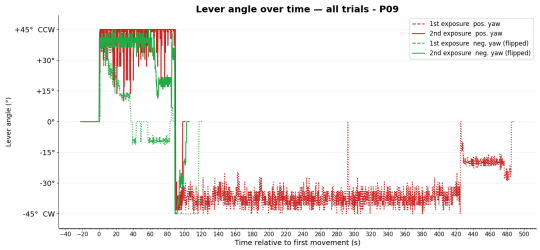

Figure A.10: Motion Perception - Lever Angle of P09

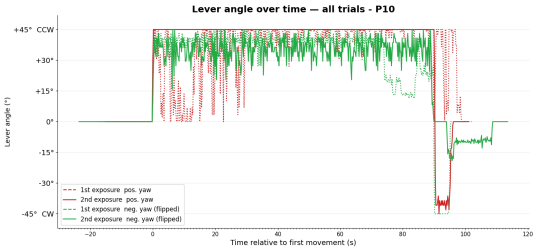

Figure A.11: Motion Perception - Lever Angle of P10

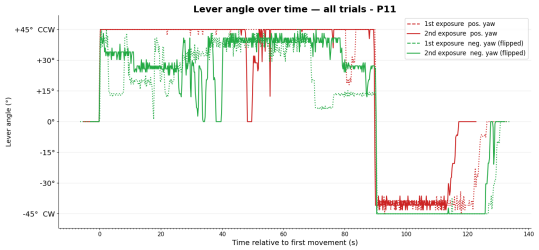

Figure A.12: Motion Perception - Lever Angle of P11

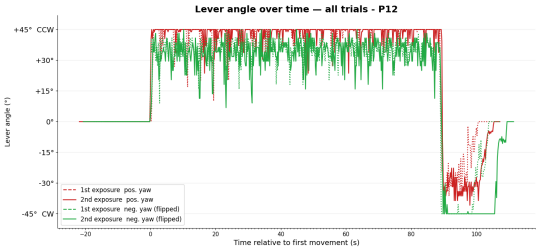

Figure A.13: Motion Perception - Lever Angle of P12

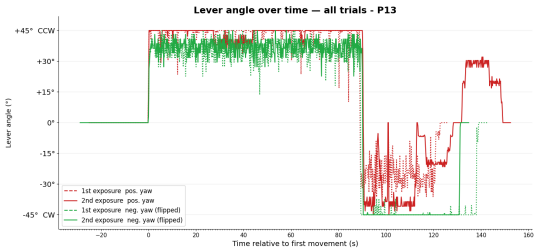

Figure A.14: Motion Perception - Lever Angle of P13

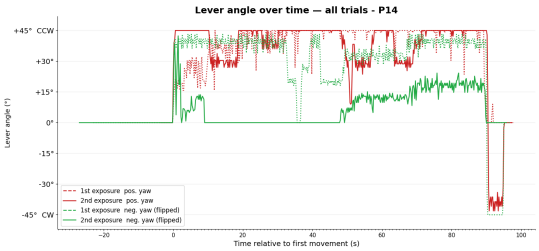

Figure A.15: Motion Perception - Lever Angle of P14

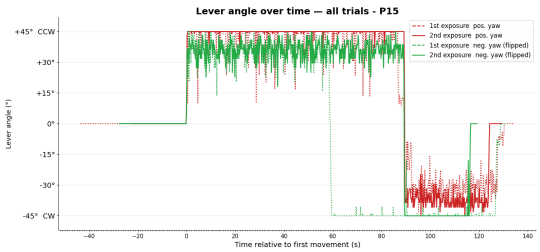

Figure A.16: Motion Perception - Lever Angle of P15

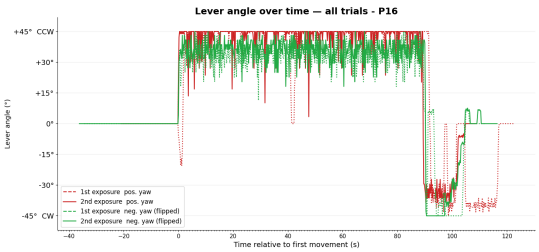

Figure A.17: Motion Perception - Lever Angle of P16

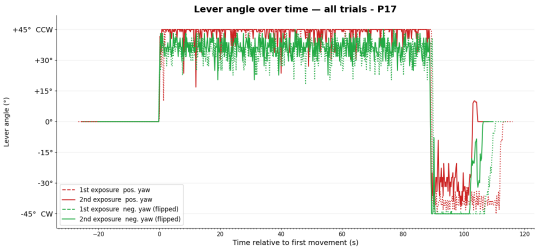

Figure A.18: Motion Perception - Lever Angle of P17

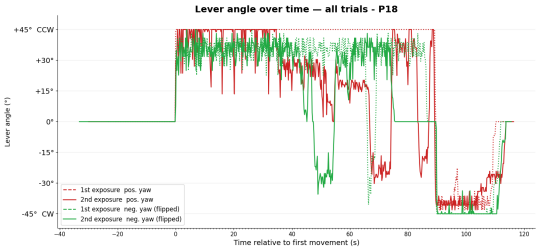

Figure A.19: Motion Perception - Lever Angle of P18

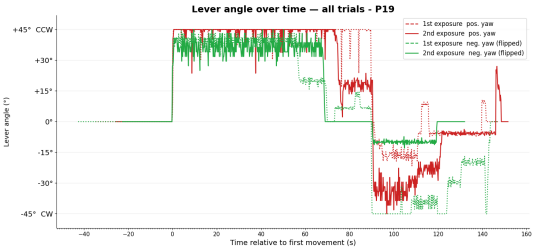

Figure A.20: Motion Perception - Lever Angle of P19

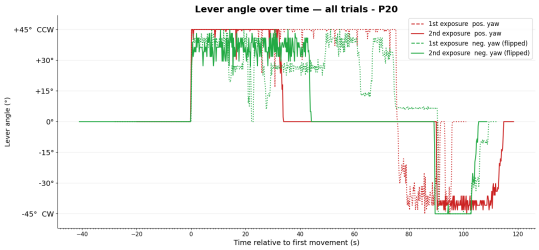

Figure A.21: Motion Perception - Lever Angle of P20

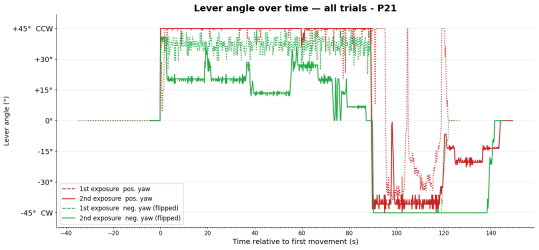

Figure A.22: Motion Perception - Lever Angle of P21

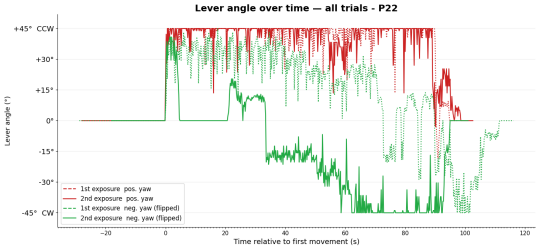

Figure A.23: Motion Perception - Lever Angle of P22

A.2. Dynamic Stabilization - Graphs

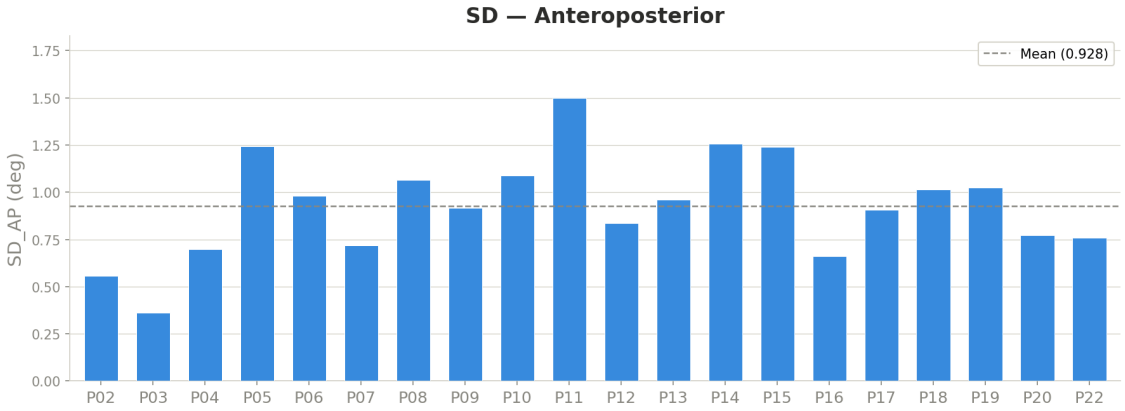

Figure A.24: SD_AP during dynamic stabilization per participant

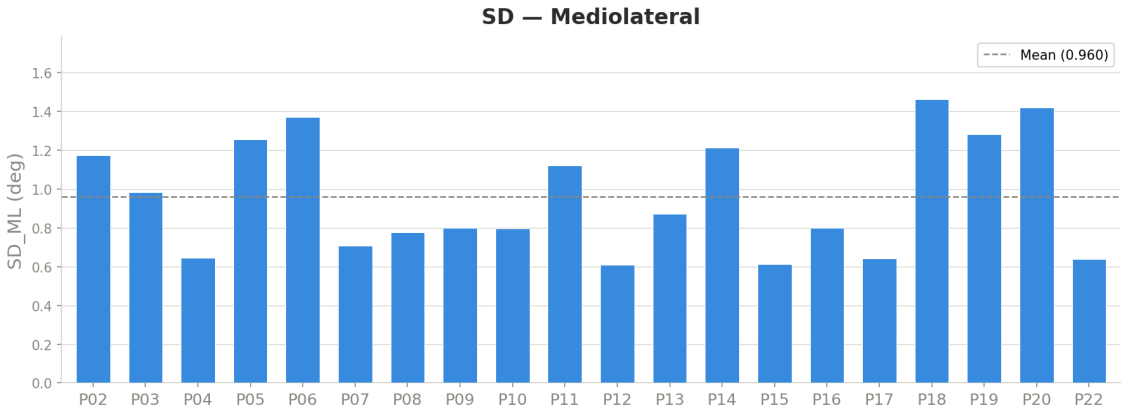

Figure A.25: SD_ML during dynamic stabilization per participant

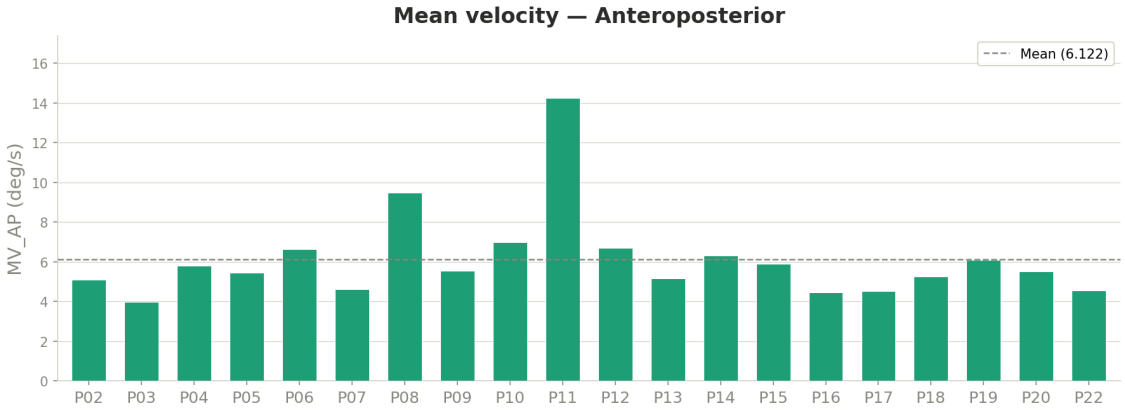

Figure A.26: MV_AP during dynamic stabilization per participant

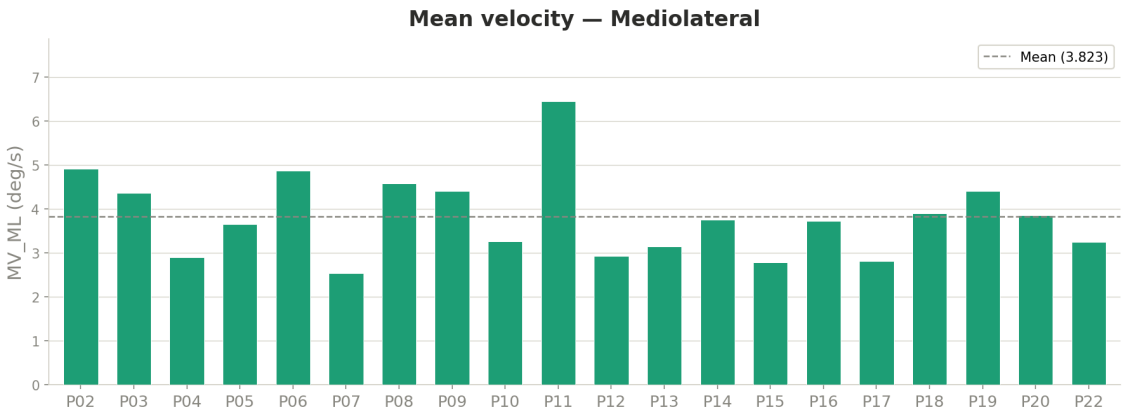

Figure A.27: MV_ML during dynamic stabilization per participant

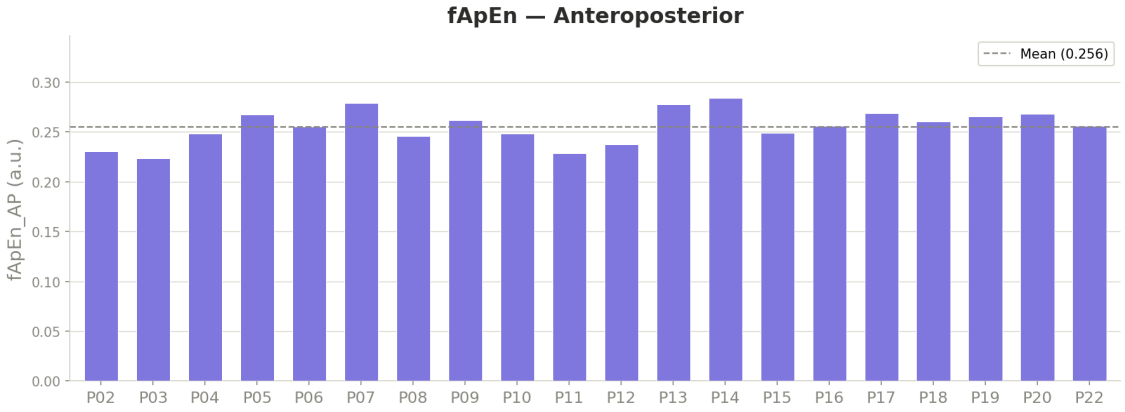

Figure A.28: fApEn_AP during dynamic stabilization per participant

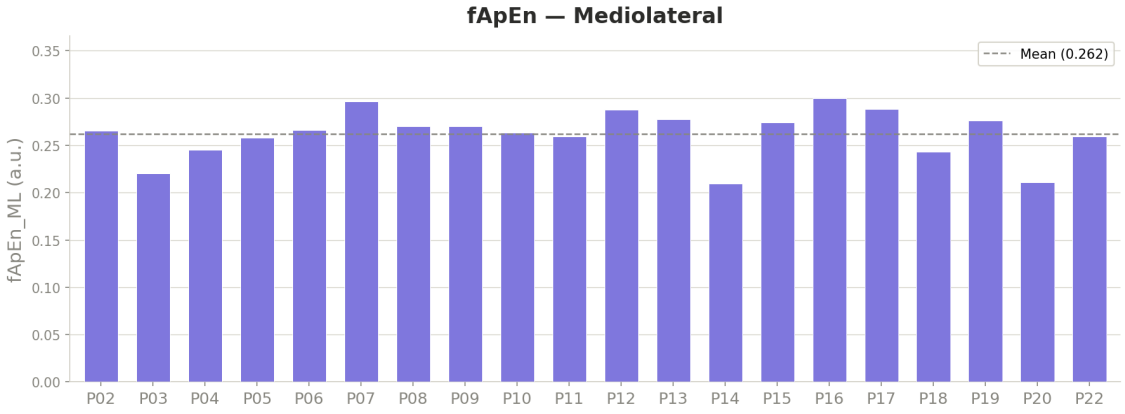

Figure A.29: fApEn_ML during dynamic stabilization per participant

A.3. Correlations - Graphs

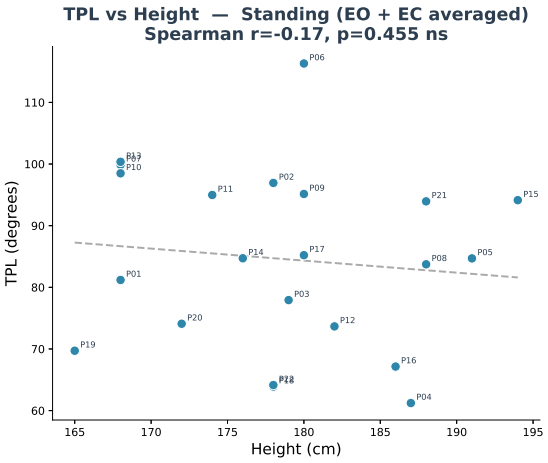

Figure A.30: Correlation between TPL during sway vs height in sitting condition

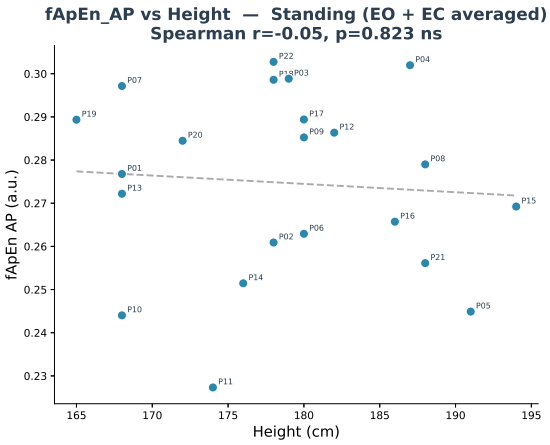

Figure A.31: Correlation between fApEn during sway vs height in sitting condition

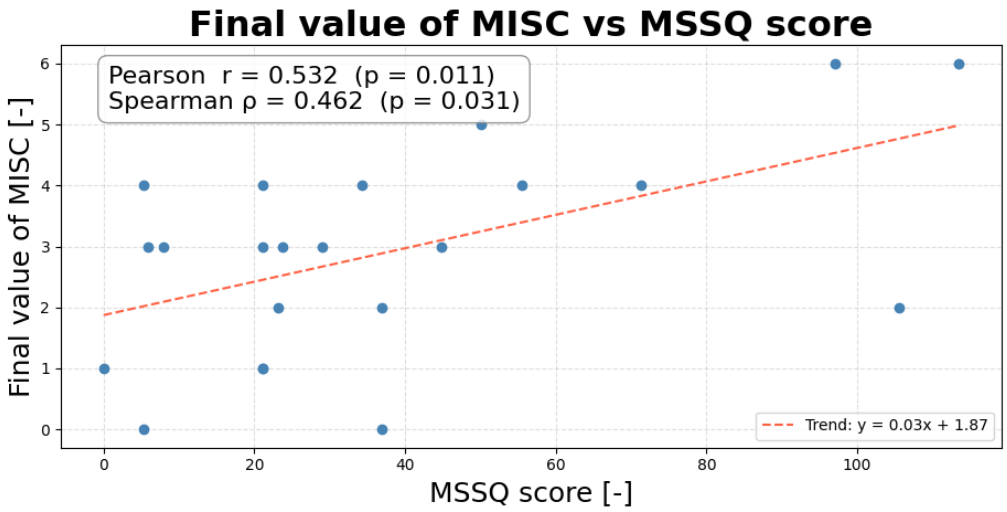

Figure A.32: Correlation between the final value of MISC and MSSQ scores

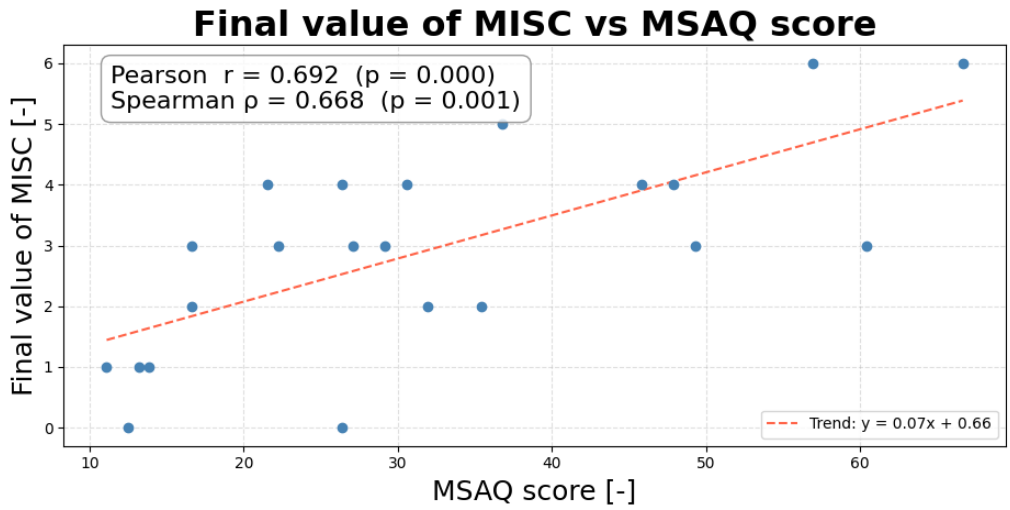

Figure A.33: Correlation between the final value of MISC and MSAQ scores

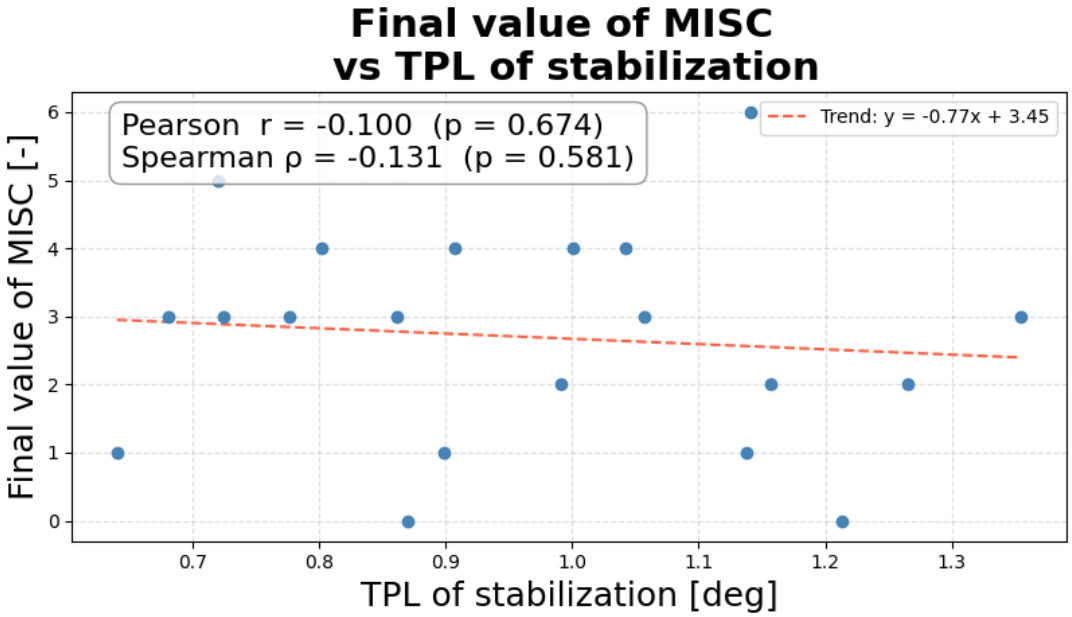

Figure A.34: Correlation between final MISC score and TPL during dynamic stabilization

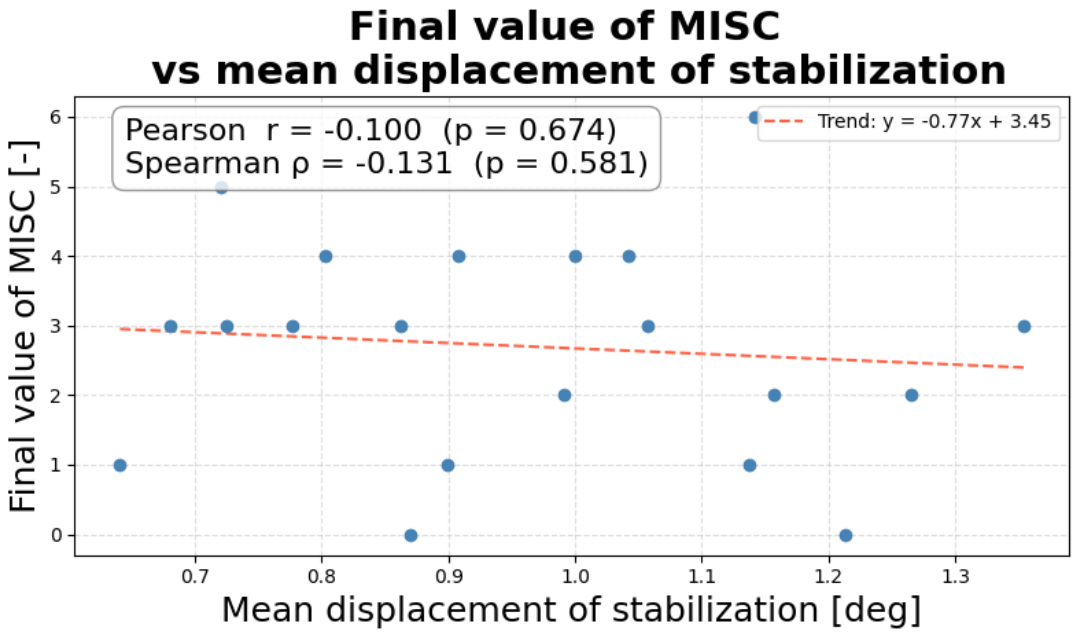

Figure A.35: Correlation between final MISC score and Mean Displacement during dynamic stabilization

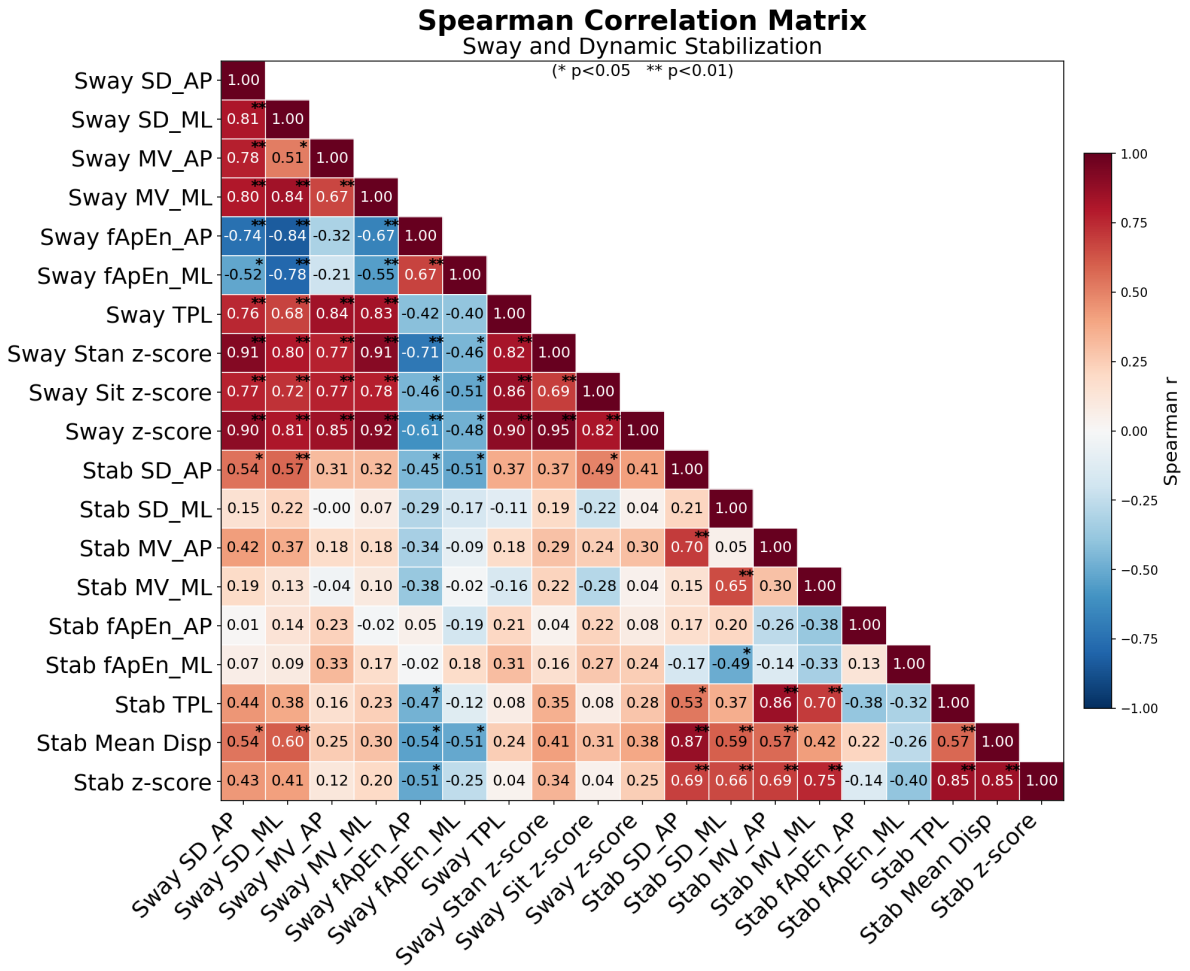

Figure A.36: Spearman correlation matrix between the postural sway and dynamic stabilization metrics, averaged across all conditions (*Stan EO, Stan EC, Sit EO, Sit EC*) and timepoints (*before & after MS exposure*) for all participants including the original P-values; p <0.05, ** p <0.01

B

Tables

B.1. Sway data

Table B.1: Overview of Spearman correlation coefficients between sway and height in both standing and sitting conditions

Metric	Standing	Sitting
SD_AP	-0.06	-0.09
SD_ML	-0.22	-0.16
MV_AP	-0.19	0.05
MV_ML	-0.18	-0.11
fApEn_AP	-0.05	0.28
fApEn_ML	0.03	0.28
TPL	-0.17	-0.02

Table B.2: Overview of z-score of sway for each participant, in the order of most sway to least sway before MS exposure; *before* MS exposure, *after* MS exposure and overall score

Participant	Before	After	Overall
P01	1.49	0.03	0.76
P06	1.31	0.47	0.90
P17	1.15	-0.22	0.41
P10	0.90	2.60	2.11
P11	0.73	0.20	0.46
P05	0.61	0.21	0.43
P13	0.52	0.44	0.52
P07	0.47	0.46	0.51
P15	0.35	0.95	0.77
P02	0.26	0.90	0.72
P21	0.17	0.69	0.50
P14	0.11	0.17	0.15
P09	0.05	-0.10	-0.05
P08	-0.11	-0.53	-0.39
P12	-0.37	-0.84	-0.71
P18	-0.77	-1.50	-1.28
P03	-0.79	-0.71	-0.84
P19	-1.02	-0.09	-0.55
P22	-1.07	-1.23	-1.28
P20	-1.12	-0.13	-0.63
P16	-1.35	-0.43	-0.94
P04	-1.50	-1.33	-1.55

Table B.3: Before-to-after ratios of postural sway metrics across all four conditions, including Spearman correlations with MISC * p<0.05, ** p<0.01, *** p<0.001, ns = not significant, including p-values; Significance Bonferroni (α = 0.005/28 = 0.00179) INCLUDING P10

Metric	Condition	Mean	SD	Test	p-value	Sign	Bonf	Spearman	p-value	Sign	Bonf
Comp. ratio	All	1.106	0.232	paired t-test	0.0438	*	n/a	0.2829	0.2021	ns	n/a
Comp. ratio	Standing	1.150	0.264	paired t-test	0.0143	*	n/a	0.3890	0.0735	ns	n/a
Comp. ratio	Sitting	1.066	0.272	Wilcoxon	0.3883	ns	n/a	0.1146	0.6115	ns	n/a
SD_AP	Stan EO	1.219	0.497	paired t-test	0.0500	*	ns	0.2411	0.2797	ns	ns
SD_AP	Stan EC	1.245	0.460	Wilcoxon	0.3535	ns	ns	0.4015	0.0640	ns	ns
SD_AP	Sit EO	1.226	0.694	Wilcoxon	0.3535	ns	ns	0.0457	0.8398	ns	ns
SD_AP	Sit EC	1.267	0.467	Wilcoxon	0.2479	ns	ns	0.1530	0.4966	ns	ns
SD_ML	Stan EO	1.473	0.636	paired t-test	0.0021	**	ns	0.2829	0.2021	ns	ns
SD_ML	Stan EC	1.248	0.461	paired t-test	0.0438	*	ns	0.3145	0.1540	ns	ns
SD_ML	Sit EO	1.136	0.567	Wilcoxon	0.9493	ns	ns	-0.1033	0.6472	ns	ns
SD_ML	Sit EC	1.281	0.463	Wilcoxon	0.1762	ns	ns	0.0762	0.7360	ns	ns
MV_AP	Stan EO	1.044	0.248	paired t-test	0.4064	ns	ns	0.2863	0.1965	ns	ns
MV_AP	Stan EC	1.130	0.299	paired t-test	0.0809	ns	ns	0.2287	0.3060	ns	ns
MV_AP	Sit EO	1.020	0.287	paired t-test	0.7462	ns	ns	0.2580	0.2463	ns	ns
MV_AP	Sit EC	1.024	0.225	paired t-test	0.6434	ns	ns	0.1440	0.5226	ns	ns
MV_ML	Stan EO	1.160	0.256	paired t-test	0.0094	**	ns	0.0401	0.8594	ns	ns
MV_ML	Stan EC	1.082	0.218	paired t-test	0.0879	ns	ns	0.3981	0.0665	ns	ns
MV_ML	Sit EO	0.982	0.204	paired t-test	0.6753	ns	ns	0.0728	0.7473	ns	ns
MV_ML	Sit EC	0.933	0.228	paired t-test	0.2018	ns	ns	0.0503	0.8242	ns	ns
fApEn_AP	Stan EO	0.986	0.215	Wilcoxon	0.0462	*	ns	-0.1259	0.5766	ns	ns
fApEn_AP	Stan EC	0.994	0.128	paired t-test	0.8582	ns	ns	-0.3066	0.1652	ns	ns
fApEn_AP	Sit EO	0.993	0.116	Wilcoxon	0.6327	ns	ns	0.0819	0.7172	ns	ns
fApEn_AP	Sit EC	1.015	0.193	Wilcoxon	0.6556	ns	ns	-0.2332	0.2963	ns	ns
fApEn_ML	Stan EO	0.929	0.149	paired t-test	0.0327	*	ns	-0.2727	0.2195	ns	ns
fApEn_ML	Stan EC	0.970	0.105	paired t-test	0.2460	ns	ns	-0.3506	0.1096	ns	ns
fApEn_ML	Sit EO	0.998	0.057	paired t-test	0.8645	ns	ns	-0.0943	0.6764	ns	ns
fApEn_ML	Sit EC	1.050	0.384	Wilcoxon	0.9240	ns	ns	-0.0164	0.9423	ns	ns
TPL	Stan EO	1.069	0.206	paired t-test	0.1257	ns	ns	0.2163	0.3337	ns	ns
TPL	Stan EC	1.024	0.253	paired t-test	0.6856	ns	ns	0.0762	0.7360	ns	ns
TPL	Sit EO	1.019	0.222	paired t-test	0.6866	ns	ns	0.2106	0.3468	ns	ns
TPL	Sit EC	0.966	0.205	paired t-test	0.4810	ns	ns	0.1587	0.4806	ns	ns

Table B.4: Before-to-after ratios of postural sway metrics across all four conditions, including Spearman correlations with MISC * p<0.05, ** p<0.01, *** p<0.001, ns = not significant, including p-values; Significance Bonferroni (α = 0.005/28 = 0.00179) EXCLUDING P10

Metric	Condition	Mean	SD	Test	p-value	Sign	Bonf	Spearman	p-value	Sign	Bonf
Comp. ratio	All	1.079	0.199	paired t-test	0.0837	ns	n/a	0.3623	0.1065	ns	n/a
Comp. ratio	Standing	1.131	0.254	paired t-test	0.0284	*	n/a	0.4610	0.0354	*	n/a
Comp. ratio	Sitting	1.029	0.214	paired t-test	0.5440	ns	n/a	0.1662	0.4714	ns	n/a
SD_AP	Stan EO	1.200	0.497	paired t-test	0.0805	ns	ns	0.2766	0.2248	ns	ns
SD_AP	Stan EC	1.123	0.460	Wilcoxon	0.5392	ns	ns	0.4896	0.0243	*	ns
SD_AP	Sit EO	1.215	0.694	Wilcoxon	0.4948	ns	ns	0.0753	0.7456	ns	ns
SD_AP	Sit EC	1.126	0.467	Wilcoxon	0.3926	ns	ns	0.1987	0.3879	ns	ns
SD_ML	Stan EO	1.499	0.636	paired t-test	0.0018	**	ns	0.2792	0.2203	ns	ns
SD_ML	Stan EC	1.183	0.461	paired t-test	0.0832	ns	ns	0.3922	0.0787	ns	ns
SD_ML	Sit EO	1.109	0.567	Wilcoxon	0.7854	ns	ns	-0.0662	0.7755	ns	ns
SD_ML	Sit EC	1.152	0.463	paired t-test	0.1487	ns	ns	0.1247	0.5903	ns	ns
MV_AP	Stan EO	1.046	0.248	paired t-test	0.4084	ns	ns	0.2909	0.2008	ns	ns
MV_AP	Stan EC	1.096	0.299	paired t-test	0.1567	ns	ns	0.3065	0.1766	ns	ns
MV_AP	Sit EO	1.020	0.287	paired t-test	0.7575	ns	ns	0.2662	0.2434	ns	ns
MV_AP	Sit EC	1.004	0.225	paired t-test	0.9355	ns	ns	0.1961	0.3942	ns	ns
MV_ML	Stan EO	1.178	0.256	paired t-test	0.0047	**	ns	0.0000	1.0000	ns	ns
MV_ML	Stan EC	1.075	0.218	paired t-test	0.1293	ns	ns	0.4429	0.0444	*	ns
MV_ML	Sit EO	0.972	0.204	paired t-test	0.5401	ns	ns	0.1299	0.5747	ns	ns
MV_ML	Sit EC	0.914	0.228	paired t-test	0.1016	ns	ns	0.0935	0.6868	ns	ns
fApEn_AP	Stan EO	0.995	0.215	Wilcoxon	0.0760	ns	ns	-0.1870	0.4170	ns	ns
fApEn_AP	Stan EC	1.014	0.128	paired t-test	0.6290	ns	ns	-0.3805	0.0888	ns	ns
fApEn_AP	Sit EO	0.996	0.116	Wilcoxon	0.4524	ns	ns	0.0403	0.8624	ns	ns
fApEn_AP	Sit EC	1.039	0.193	Wilcoxon	0.4120	ns	ns	-0.3013	0.1844	ns	ns
fApEn_ML	Stan EO	0.930	0.149	paired t-test	0.0448	*	ns	-0.3091	0.1728	ns	ns
fApEn_ML	Stan EC	0.982	0.105	Wilcoxon	0.3038	ns	ns	-0.4325	0.0502	ns	ns
fApEn_ML	Sit EO	1.004	0.057	Wilcoxon	0.7938	ns	ns	-0.1753	0.4472	ns	ns
fApEn_ML	Sit EC	1.078	0.384	Wilcoxon	0.6578	ns	ns	-0.0623	0.7884	ns	ns
TPL	Stan EO	1.076	0.206	paired t-test	0.1038	ns	ns	0.2234	0.3304	ns	ns
TPL	Stan EC	0.998	0.253	paired t-test	0.9720	ns	ns	0.1416	0.5405	ns	ns
TPL	Sit EO	1.016	0.222	paired t-test	0.7501	ns	ns	0.2351	0.3050	ns	ns
TPL	Sit EC	0.946	0.205	paired t-test	0.2446	ns	ns	0.2091	0.3630	ns	ns

Table B.5: Before and After timepoints averaged per condition, Mean, SD and CV (= SD/Mean) in the standing conditions

	Stan EO			Stan EC		
	Mean	**SD**	**CV**	**Mean**	**SD**	**CV**
SD_AP (°)	0.251	0.099	0.394	0.300	0.126	0.420
SD_ML (°)	0.198	0.101	0.510	0.189	0.078	0.413
MV_AP (°/s)	0.741	0.159	0.215	0.780	0.215	0.276
MV_ML (°/s)	0.615	0.161	0.262	0.627	0.157	0.250
fApEn_AP (a.u.)	0.279	0.030	0.108	0.273	0.029	0.106
fApEn_ML (a.u.)	0.282	0.032	0.113	0.287	0.022	0.077
TPL (°)	82.49	15.69	0.190	85.42	22.60	0.265

Table B.6: Before and After timepoints averaged per condition, Mean, SD and CV (= SD/Mean) in the sitting conditions

	Sit EO			Sit EC		
	Mean	**SD**	**CV**	**Mean**	**SD**	**CV**
SD_AP (°)	0.131	0.054	0.412	0.122	0.058	0.475
SD_ML (°)	0.099	0.042	0.424	0.099	0.057	0.576
MV_AP (°/s)	0.476	0.135	0.284	0.454	0.126	0.278
MV_ML (°/s)	0.391	0.094	0.240	0.351	0.080	0.228
fApEn_AP (a.u.)	0.289	0.024	0.083	0.289	0.028	0.097
fApEn_ML (a.u.)	0.287	0.019	0.066	0.285	0.036	0.126
TPL (°)	53.78	12.46	0.232	49.14	13.52	0.275

B.2. Stabilization data

Table B.7: Parameter summary of stabilization results per participant

Metric	SD_AP	SD_ML	MV_AP	MV_ML	fApEn_AP	fApEn_ML	TPL	MeanDisp	Comp. index
	(deg)	(deg)	(deg/s)	(deg/s)	(a.u.)	(a.u.)	(deg)	(deg)	(z-score)
P02	0.5573	1.1730	5.1061	4.9061	0.2306	0.2653	1674.255	0.8620	0.005
P03	0.3612	0.9829	3.9752	4.3598	0.2232	0.2203	1442.681	0.6407	-0.569
P04	0.6964	0.6447	5.8088	2.8951	0.2483	0.2454	1518.973	0.6808	-0.664
P05	1.2419	1.2578	5.4641	3.6569	0.2673	0.2582	1502.041	1.2651	0.273
P06	0.9801	1.3719	6.6505	4.8679	0.2555	0.2662	1851.227	1.1565	0.647
P07	0.7185	0.7093	4.6332	2.5420	0.2793	0.2967	1151.512	0.7209	-0.922
P08	1.0646	0.7778	9.4828	4.5821	0.2458	0.2702	2395.774	1.0004	0.708
P09	0.9178	0.8007	5.5653	4.4006	0.2617	0.2705	1673.884	0.8995	-0.043
P10	1.0867	0.7975	6.9915	3.2582	0.2484	0.2637	1771.771	0.9913	0.004
P11	1.4994	1.1213	14.2595	6.4479	0.2283	0.2596	3607.537	1.3545	2.533
P12	0.8349	0.6084	6.7114	2.9291	0.2374	0.2875	1666.346	0.7765	-0.443
P13	0.9599	0.8736	5.1562	3.1435	0.2777	0.2774	1378.372	0.9073	-0.375
P14	1.2567	1.2152	6.3075	3.7483	0.2842	0.2095	1727.223	1.2133	0.435
P15	1.2409	0.6133	5.8908	2.7778	0.2491	0.2740	1492.089	1.0576	-0.31
P16	0.6614	0.7990	4.4758	3.7237	0.2563	0.2999	1323.678	0.8024	-0.605
P17	0.9057	0.6423	4.5396	2.8163	0.2689	0.2882	1225.167	0.8701	-0.751
P18	1.0157	1.4638	5.2522	3.8945	0.2605	0.2435	1499.542	1.1379	0.274
P19	1.0251	1.2813	6.0790	4.3987	0.2658	0.2764	1725.057	1.1415	0.423
P20	0.7705	1.4217	5.5186	3.8600	0.2680	0.2110	1583.739	1.0419	0.112
P22	0.7581	0.6382	4.5716	3.2519	0.2563	0.2596	1318.634	0.7252	-0.733
Mean	0.928	0.960	6.122	3.823	0.256	0.262	1676.48	0.962	0
SD	0.27	0.30	2.26	0.95	0.017	0.026	527.9	0.21	0.774
Min	0.361	0.608	3.975	2.542	0.223	0.210	1151.51	0.640	-0.922
Max	1.499	1.464	14.26	6.448	0.284	0.299	3607.54	1.355	2.533
SD/Mean	0.291	0.313	0.369	0.249	0.066	0.099	0.315	0.218	-

Table B.8: Mean and SD of each stabilization metric, including Spearman correlations with MISC score
* p<0.05, ** p<0.01, *** p<0.001, ns = not significant, including p-values
INCLUDING P11

Metric	Unit	Mean	SD	Spearman	p-value	Sign
SD_AP	(deg)	0.9276	0.2701	0.1203	0.6134	ns
SD_ML	(deg)	0.9597	0.2986	-0.1113	0.6405	ns
MV_AP	(deg/s)	6.1220	2.2636	0.2526	0.2826	ns
MV_ML	(deg/s)	3.8230	0.9528	0.0060	0.9799	ns
fApEn_AP	(a.u.)	0.2556	0.0170	-0.0662	0.7816	ns
fApEn_ML	(a.u.)	0.2622	0.0256	0.3558	0.1237	ns
TPL	(deg)	1676.4752	527.9306	0.1173	0.6224	ns
MeanDisp	(deg)	0.9623	0.2064	0.1188	0.6179	ns

Table B.9: Mean and SD of each stabilization metric, including Spearman correlations with MISC score
* p<0.05, ** p<0.01, *** p<0.001, ns = not significant, including p-values
EXCLUDING P11

Metric	Unit	Mean	SD	Spearman	p-value	Sign
SD_AP	(deg)	0.8975	0.2406	-0.0158	0.9488	ns
SD_ML	(deg)	0.9512	0.3043	-0.1737	0.477	ns
MV_AP	(deg/s)	5.6937	1.2394	0.1386	0.5715	ns
MV_ML	(deg/s)	3.6849	0.7452	-0.1509	0.5375	ns
fApEn_AP	(a.u.)	0.2571	0.0162	0.0369	0.8809	ns
fApEn_ML	(a.u.)	0.2623	0.0263	0.4211	0.0726	ns
TPL	(deg)	1574.8403	275.9067	-0.0211	0.9318	ns
MeanDisp	(deg)	0.9416	0.1897	-0.0211	0.9318	ns

C

MSSQ

C.1. Motion Sickness Susceptibility Questionnaire

Background Questions

1. Please state your age

   ... *years*

2. Please state your sex

   Male - Female - Other

3. Please state your height

   ... *cm*

4. Please state your current weight

   ... *kg*

5. Do you have any medical impairments? If so, please explain

   No - Yes, namely ...

6. Do you regard yourself as susceptible to motion sickness?

   Not at all - Slightly - Moderately - Very much so

A. Childhood Experience (before age of 12 years)

5. As a Child (before 12 years), how often you travelled or experienced:

	Never	1 to 4 trips	5 to 10 trips	11 or more trips
Cars				
Buses or Coaches				
Trains				
Aircraft				
Small Boats				
Ships, e.g. Channel Ferries				
Swings				
Roundabouts: playgrounds				
Big Dippers, Funfair Rides				

6. As a Child (before 12 years), how often you felt sick or nauseated:

	Never	Rarely	Sometimes	Frequently	Always
Cars					
Buses or Coaches					
Trains					
Aircraft					
Small Boats					
Ships, e.g. Channel Ferries					
Swings					
Roundabouts: playgrounds					
Big Dippers, Funfair Rides					

7. As a Child (before 12 years), how often you vomited:

	Never	Rarely	Sometimes	Frequently	Always
Cars					
Buses or Coaches					
Trains					
Aircraft					
Small Boats					
Ships, e.g. Channel Ferries					
Swings					
Roundabouts: playgrounds					
Big Dippers, Funfair Rides					

B. Adult Experience (over the last 10 years)

8. Over the last 10 years, how often you travelled or experienced:

	Never	1 to 4 trips	5 to 10 trips	11 or more trips
Cars				
Buses or Coaches				
Trains				
Aircraft				
Small Boats				
Ships, e.g. Channel Ferries				
Swings				
Roundabouts: playgrounds				
Big Dippers, Funfair Rides				

9. Over the last 10 years, how often you felt sick or nauseated:

	Never	Rarely	Sometimes	Frequently	Always
Cars					
Buses or Coaches					
Trains					
Aircraft					
Small Boats					
Ships, e.g. Channel Ferries					
Swings					
Roundabouts: playgrounds					
Big Dippers, Funfair Rides					

10. Over the last 10 years, how often you vomited:

	Never	Rarely	Sometimes	Frequently	Always
Cars					
Buses or Coaches					
Trains					
Aircraft					
Small Boats					
Ships, e.g. Channel Ferries					
Swings					
Roundabouts: playgrounds					
Big Dippers, Funfair Rides					

D

MSAQ

D.1. Motion Sickness Assessment Questionnaire

Using the scale below, please rate how accurately the following statements describe your experience.

Not at all								Severely
1	2	3	4	5	6	7	8	9

1. I felt sick to my stomach (G)
2. I felt faint-like (C)
3. I felt annoyed/irritated (S)
4. I felt sweaty (P)
5. I felt queasy (G)
6. I felt lightheaded (C)
7. I felt drowsy (S)
8. I felt clammy/cold sweat (P)
9. I felt disoriented (C)
10. I felt tired/fatigued (S)
11. I felt nauseated (G)
12. I felt hot/warm (P)
13. I felt dizzy (C)
14. I felt like I was spinning (C)
15. I felt as if I may vomit (G)
16. I felt uneasy (S)

NOTE:

- *G: Gastrointestinal*
- *C*: *Central*
- *P*: *Peripheral*
- *S*: *Sopite-related*

The overall motion sickness score is obtained by calculating the percentage of total points scored:

$$\text{Overall score} = \frac{\text{sum of points from all items}}{144} \times 100 \tag{D.1}$$

Subscale scores are obtained by calculating the percent of points scored within each factor:

$$\text{Gastrointestinal} = \frac{\text{sum of gastrointestinal items}}{36} \times 100 \tag{D.2}$$

$$\text{Central} = \frac{\text{sum of central items}}{45} \times 100 \tag{D.3}$$

$$\text{Peripheral} = \frac{\text{sum of peripheral items}}{27} \times 100 \tag{D.4}$$

$$\text{Sopite-related} = \frac{\text{sum of sopite-related items}}{36} \times 100 \tag{D.5}$$

E

MISC

E.1. Misery Scale (MISC)

Table E.1: MIsery SCale (MISC) and associated symptoms. [de Winkel et al., 2022]

MISC score	Symptoms
0	No problems
1	Uneasiness
2	Vague dizziness, warmth, headache, stomach awareness, sweating
3	Slight dizziness, warmth, headache, stomach awareness, sweating
4	Fair dizziness, warmth, headache, stomach awareness, sweating
5	Severe dizziness, warmth, headache, stomach awareness, sweating
6	Slight nausea
7	Fair nausea
8	Severe nausea
9	(Near) retching
10	Vomiting

F

Instructions Experiments

F.1. Introduction

“The experiment consists of 7 different experiments and will take around 2 hours to complete. Here is the participation info and consent form. You are allowed to withdraw at any time without having to give a reason. The purpose of this study is to find individual differences in posture, sway, and motion sickness. Only at the end, an experiment is conducted to test your susceptibility to motion sickness. But I will monitor your well-being constantly during the other experiments as well to make sure everything goes well.”

TO DO

- Give consent form and sign it (both parties)

F.2. MSSQ

“We will start with a questionnaire (Motion Sickness Susceptibility Questionnaire) consisting of general questions about yourself and questions regarding your motion experience in the past.”

TO DO

- Give questionnaire (done online)

F.3. Standing Sway

“The first experiment is the *standing* sway test. You have to stand straight, with your feet shoulder-width apart and your hands by your sides. You have to look forward and keep this for 90 seconds while focusing on stabilizing. You will have to repeat this with your eyes closed.”

TO DO

- Check stance
- Tell them to focus on stabilizing
- Put the sensor on the head
- Start recording
- Repeat with a blindfold

F.4. Sitting sway

“The second experiment is the sitting sway test. You have to sit straight, with your head straight and your hands on your thighs. You have to look forward and keep this for 90 seconds while focusing on

stabilizing. You will have to repeat this with your eyes closed."

TO DO

- Check stance
- Tell them to focus on stabilizing
- Put the sensor on the head
- Start recording
- Repeat with a blindfold

F.5. Motion Perception Test

"The next experiment is the motion perception test. You can take a seat in the chair, secure yourself well, and place your feet on the stands. You will have to put on a blindfold and headphones to mitigate external input. You also have to put a sensor on your head.
We start with a control experiment; I will play a sound, and you have to move the lever so that you perceive the sound decreasing. Next, you can take a seat in the chair and secure yourself well and place your feet on the stands. You will have to put on the glasses and headphones to mitigate external input. You have to take the controller in your hand and with the lever you have to indicate how you perceive the rotation velocity. First, you will be turned in one direction, and you can move the stick fully in that direction. When you feel the velocity reducing, you can turn the stick proportionally towards the neutral position. When the movement direction changes, you have to change the stick in the corresponding direction. If you do not feel movement, you can put the lever in neutral. You need to indicate the motion you feel, not the motion you think is happening. If the music stops, you can take a 30-second break and take off the glasses. You need to keep your head against the headrest, otherwise you might get sick. We will repeat this 4 times. You can stop at any time if you do not feel comfortable. Are there any questions?"

TO DO

- Make sure participant is secured
- Put on a blindfold and headphones
- Put on sensors (head and seat)
- Turn chair while recording response
- Repeat 4 times, twice in each direction

F.6. Motion sickness

"This experiment consists of a driving scenario with 240-second laps, followed by a 10-second break, which is repeated 6 times. Your motion sickness level will be measured every 30 seconds, with a prompt via an auditory beep through the headphones. The level of sickness will be determined using the MISC and will be stopped immediately when you reach a score of 6."

TO DO

- Explain MISC score
- Check position in the simulator
- Start recording

F.7. Standing Sway

"We will repeat the standing sway test the same as before. We will repeat this again with eyes closed."

TO DO

- Check stance
- Instruct to keep head to minimize sway
- Put the sensor on the head
- Start recording

F.8. Sitting sway

“We will repeat the standing sway test the same as before. We will repeat this with eyes closed.”

TO DO

- Check stance
- Instruct to keep head to minimize sway
- Put the sensor on the head
- Start recording

F.9. MSAQ

“We will end the experiment with a (Motion Sickness Assessment) questionnaire consisting of 16 statements where you have to rate the accuracy from 1 to 9.”

TO DO

- Hand out MSAQ